Interim Technical Report

on

NAG 5-510

ESTIMATION OF VEGETATION COVER AT SUBPIXEL RESOLUTION USING LANDSAT DATA

by

Michael F. Jasinski

Research Assistant

and

Peter S. Eagleson

Edmund K. Turner Professor of Civil Engineering

Principal Investigator

Department of Civil Engineering

Massachusetts Institute of Technology

Cambridge, Massachusetts 02139

1 June 1986 through 30 November 1986

CONTENTS

Introduction

This report summarizes progress made from 1 June 1986 through 30 November 1986 in developing an effective algorithm for estimating vegetation cover at subpixel resolution. An important application is the estimation of soil hydraulic properties in natural water-limited vegetation systems using Eagleson's "climatic-climax" hypothesis (Eagleson, 1982, Eagleson and Tellus, 1982). It is also critical to the subgrid-scale parameterization of heat and moisture fluxes across the atmosphere-landsurface interface in the development of global-scale numerical atmospheric general circulation models (GCMs). Such models are essential for the study of climate change and for large-scale environmental impact assessment. Calculation of the fluxes requires knowledge of effective areal averages of soil hydraulic properties and of vegetation characteristics at the mesoscale.

An earlier report (Jasinski and Eagleson, April 1986) concluded that only a few methods for resolving mixed pixels were available, and they had not been tested for the special case of determining percent canopy cover. Two formulations were proposed: One using the normalized vegetation index, a second involving a simplified expression of the radiative transfer equation.

That report also includes details of the database acquired for the project study area near Taos, New Mexico. Landsat MSS data were obtained from the Bureau of Land Management (BLM) Branch of Remote Sensing, Denver, Colorado. Ground truth in the form of 1:3000 color aerial photographs were borrowed from the BLM Taos Resource Area Office, Taos, New Mexico.

The present report summarizes the various approaches relevant to estimating canopy cover at subpixel resolution. The approaches are based on physical models of radiative transfer in non-homogeneous canopies and on empirical methods. The effects of vegetation shadows and topography are examined. Simple versions of the model are tested, using the Taos Study Area database. Emphasis has been placed on using relatively simple models requiring only one or two bands. Although most methods require some degree of ground truth, a two-band method is investigated whereby the percent cover can be estimated without ground truth by examining the limits of the data space. Future work is proposed which will incorporate additional surface parameters into the canopy cover algorithm, such as topography, leaf area, or shadows. The method involves deriving a probability density function for the percent canopy cover based on the joint probability density function of the observed radiances.

Homogeneous Canopy Reflectance

The radiation reflected from horizontally homogeneous canopies results from the scattering and reflectance properties of the plant components and soil background. These properties are both geometric and biophysical in nature and thus depend on the species, maturity and overall health of the plant. Geometric plant properties include plant architecture, total leaf area, and leaf orientation and distribution. Biophysical properties allocate the radiative energy absorbed by the plant to important metabolic processes including photosynthesis, respiration, and transpiration. Those biophysical properties are manifested in terms of leaf color, transparency, temperature, and shape and orientation. Plant properties can vary daily and seasonally, in response to soil moisture and nutrients, and to meteorologic and climatic conditions.

Numerous radiative transfer models for horizontally homogeneous canopies have been developed in terms of various plant properties and background soil reflectance. Typically, homogeneous canopies have been modeled as a diffusing medium with absorbing and scattering properties. Excellent reviews of these models are provided by Smith (1983) and Ross (1984). Suits (1972) envisioned a plant canopy as an infinitely extended plane-parallel medium with homogeneous geometric properties. Verhoeff and Bunnik (1981) extended the soils model to include the effect of leaf angle distribution. Dickinson (1983) applied the two-stream approximation for radiation transfer in the atmosphere (Meador et al., 1980) to plant canopies employing the leaf area index (LAI) as a measure of the optical depth. Recent literature has increased the sophistication of those earlier models to include the modeling of bidirectional reflectance (Walthall et al., 1985, Chen, 1985, Simmer et al., 1985, Vanderbilt et al., 1985, Strebel et al., 1985, Gerstl et al., 1985, and Reyna et al., 1985). Attention has also been focused on the invertibility of canopy reflectance models for estimating plant parameters such as LAI, biomass, and leaf angle distribution (LAD) (Goel et al., 1983, Goel et al., 1984a, Goel et al., 1984b, 1984c, 1984d, Lang et al., 1985). Goel et al. (1984) have shown that such parameters can, in principle, be estimated using only canopy reflectance measurements at several viewing angles.

Because such theoretical models are often cumbersome to use, semi-empirical formulas for the total radiation fluxes have been proposed for practical applications. The attenuation of radiation as it passes through a plant stand has been typically described in terms of some form of Bouguer's Law such as that proposed by Monsi and Saeki (1953), or

$$I(L) = I_o \exp(-\mu L) \qquad (1)$$

where

I_o = intensity of radiation at top of canopy

$I(L)$ = intensity of radiation at a penetration level associated with leaf area index, L

μ = experimentally determined extinction coefficient

The plant reflectance, r_v, is thus

$$r_v = 1 - e^{-\mu L} \qquad (2)$$

Other formulas which account for the different attenuation of penetrated and scattered radiation, as well as absorbed radiation, have been proposed (Ross, 1981).

Actual reflectances of plants in the visible and near infrared are well documented, especially for crops (Smith, 1983, Myers, 1983). Canopy reflectance is highly wavelength dependent as shown in Exhibit 1. It is typically low in the visible spectrum (< 30%) and higher in the near infrared region (> 50%). Canopy reflectances are generally much lower than those measured for individual leaves (Dickinson, 1983). Kondratyev (1969), Gates (1980), Ross (1981) and Iqbal (1983) provide summaries of reflectances for various natural vegetation covers.

Non-Homogeneous Canopy Reflectance

Non-homogeneous canopies are those which contain several vegetation or soil types within the level of resolution being investigated. Most natural landscapes will vary both horizontally and vertically in species and/or vegetation density. Modeling this situation has received considerably less attention than have homogeneous canopies. Statistical techniques have been employed for classifying landscapes. However, such methods require the identification of training samples and therefore can

not be adopted for natural landscapes in which all target pixels possess unique spectral characteristics.

Radiative transfer models for non-homogeneous canopies have been developed by extending homogeneous canopy models and including three-dimensional scattering functions (Ross, 1981, Kimes, 1984). Such models can be solved in a few cases where plant distribution is periodic, such as for sown crops. Applications to natural systems is impractical if not impossible as it would require knowing a priori an inordinate number of plant parameters.

The problem can be somewhat simplified by recognizing that for most hydrologic or climate modeling purposes, it is generally sufficient to know only the outgoing radiance at the surface of a canopy, and not the complex scattering and absorption phenomena within the canopy.

Researchers have investigated mixed pixels by examining only the surface reflectivities of the individual components. Two such approaches are summarized below.

Proportion Estimation

A simple approach has been to assume that the surface reflectivities of individual plant clusters and soils within a pixel are constant, and that the total spectral response is a linear combination of the individual spectral responses of its components (Horwitz et al., 1971, Nalepka et al., 1972, Work, 1974, McCloy, 1980, Dozier, 1981, Ungar et al., 1981, Chhikara, 1984). The total radiance emitted from a pixel, I_λ, containing n cover types can be expressed

$$I_\lambda = \sum_{i=1}^{n} m_i I_{\lambda i} \qquad (3)$$

where

m_i = fraction of area covered by cover type i;

$I_{\lambda i}$ = radiance emitted from cover type i in band λ.

For the simple case of vegetation and soil cover, each with constant reflectivities, Equation (3) becomes:

$$I_\lambda = mI_{\lambda v} + (1-m)I_{\lambda s} \quad (4)$$

m = percent vegetation cover

$I_{\lambda v}, I_{\lambda s}$ = radiances emitted from vegetation and soil, respectively, in band λ.

Perhaps the earliest development of proportion estimation can be attributed to Horwitz et al. (1971) and Nalepko et al. (1977) who also termed the method "mixtures estimation". One of its first applications was in identifying subpixel scale ponding and wet marshes in glaciated prairies (Work, 1974).

McCloy (1980) later proposed that under conditions of negligible canopy transmission or multiple reflection, the response proportions of the various land covers will closely approximate the physical proportions of each type of cover. He suggested that up to four sub-pixel categories be used including three levels of vegetation greenness cover and one soil background cover. Ungar et al. (1981) reported limited success delineating forest canopy types in Maine using a similar approach which they termed the "Fanning algorithm". The functional area was determined by minimizing the error between observed and theoretical radiances.

Dozier (1981) also proposed such a method using two infrared bands for differentiating radiant temperature fields of sub-pixel spatial resolution. Corrections for atmospheric effects were included.

Geometric Models

In an extension to the linear proportion estimation model described above, some investigators have considered the shadow cast by vegetation as an additional component to the total radiance. These models abstract clumps of vegetation as three-dimensional geometric shapes on horizontal surfaces with constant reflectivities (Otterman 1981, 1984, Otterman et al., 1984, Strahler et al., 1981, Li et al., 1985).

Otterman (1981, 1984) and Otterman et al. (1984) envisioned forests and desert vegetation as thin vertical cylinders. While accounting for the shadowing effects of vegetation clumps, the formulation assumes that reflection from the top of the clumps is negligible. This model is thus not directly applicable to the determination of percent vegetation cover.

Strahler et al. (1981) and Li et al. (1985) modeled conifer forests as randomly located cones of similar shape and random height. They determined from simple geometry the shadow cast by the cones on the soil background or on other cones. The total radiance emitted by a pixel was assumed to consist of four components: illuminated background, illuminated cones, shadowed background and shadowed cones. Vegetation parameters including percent cover and average tree height were then estimated using assumed values of component reflectivities.

A simple version of the geometric model is presented below. Assuming the radiance emitted from shadowed areas negligible, the total radiance from sparse conifer trees, I_λ, modeled as cones on a horizontal soil background with constant reflectivities is,

$$I_\lambda = I_{\lambda o}\{m[r_{\lambda v}(\frac{1}{2} + \frac{\gamma}{\pi}) - r_{\lambda s}(\frac{1}{2} + \frac{\cot \gamma}{\pi} + \frac{\gamma}{\pi})] + r_{\lambda s}\} \qquad (5)$$

$$\gamma = \sin^{-1}(\tan \alpha / \tan \theta)$$

θ = solar zenith angle

α = ratio of tree height to base radius, assumed to be constant

$I_{\lambda o}$ = incident radiation in band λ.

The model can be extended to include non-horizontal surfaces and overlapping of shadows. Li et al. (1985) further assumed a poisson distribution of the cones and random overlap of shadows.

Satellite Observed Radiance

In order to derive canopy parameters from satellite data, it is necessary to couple the radiative transfer through the atmosphere to that through the plant canopy. As a starting point, it is useful to review the atmospheric models which have been developed for the visible and near infrared regions.

The theoretical nadir radiance observed by a satellite has been derived by several authors (Dave 1980, Otterman et al., 1979, 1980, and Otterman, 1978, 1981) for a pure pixel in a background of different reflectivity. The nadir radiance is expressed in terms of three components. The direct beam from the object pixel which has been attenuated due to atmospheric effects, $L_{nr\lambda}$, is

$$L_{nr\lambda} = rG_{\lambda} \exp(-\tau_{\lambda})/\pi \qquad (6)$$

where r = reflectivity of object pixel

G_{λ} = global surface irradiance on object pixel (Otterman, 1978)

τ_{λ} = total vertical optical thickness, a function of λ.

The total optical thickness is a sum of optical thicknesses due to Rayleigh scattering by gas molecules, τ_R, and Mie scattering by aerosols,

τ_M, also functions of λ.

Assuming a Lambertian surface, the portion of diffuse radiance from the surrounding vicinity which is scattered to the satellite by the atmospheric column above the object pixel is

$$L_{na\lambda} = (aG_\lambda/\pi\tau_\lambda)\int_o^{\pi/2} [1-\exp(-\tau_\lambda/\cos\phi)]\cos\phi[\tau_{\lambda R}P_{\lambda R}(\phi)+\tau_{\lambda M}P_{\lambda M}(\phi)]2\pi\sin\phi d\phi \quad (7)$$

where

a = average reflectivity of the surrounding vicinity

$P_{\lambda R}, P_{\lambda M}$ = phase functions associated with Rayleigh and aerosol (Mie) scattering, respectively

ϕ = zenith reflection angle.

Finally, the radiance scattered from the direct solar beam back to the satellite is written

$$L_{nd\lambda} = \frac{\mu\,[1-\exp\{-\tau_\lambda(1+\sec\theta)\}][\tau_{\lambda R}P_{\lambda R}(180^\circ-\theta) + \tau_{\lambda M}P_{\lambda M}(180^\circ-\theta)]}{\tau_\lambda(1+\mu)} \quad (8)$$

where $\mu = \cos\theta$

θ = solar zenith angle

The total nadir radiance is the sum of equations (6), (7) and (8). The amount of area to be considered in determining the average surrounding reflectivity is discussed by Otterman et al. (1979). Otterman et al. (1980) reduced the above equations to a simpler form in the case of an optically thin atmosphere.

Subpixel Resolution of Satellite Observed Radiance

The atmospheric model is coupled to the canopy models through the reflectance parameter, r, in the direct beam equation. For homogeneous canopies, the direct beam equation can be rewritten for example,

$$L_{nr\lambda} = \frac{G_\lambda}{\pi} \left(1 - e^{-\mu L}\right) e^{-\tau_\lambda} \tag{9}$$

For non-homogeneous landscapes, the proportion estimation equation (3) can be included into the direct beam equation yielding

$$L_{nr\lambda} = \frac{G_\lambda}{\pi} \exp\left(-\tau_\lambda\right) \left[\sum_{i=1}^{n} m_i r_{\lambda i}\right] \tag{10}$$

where r_i = reflectivity of component i

m_i = fraction of pixels exhibiting reflectance $r_{\lambda i}$.

Finally, the conical geometric model incorporated into the direct beam equation yields

$$L_{nr\lambda} = \frac{G_\lambda}{\pi} \exp(-\tau_\lambda)\{[m(r_{\lambda v}(\tfrac{1}{2} + \tfrac{\gamma}{\pi}) - r_{\lambda s}(\tfrac{1}{2} + \frac{\cot\gamma}{\pi} + \tfrac{\gamma}{\pi}))] + r_{\lambda s}\} \tag{11}$$

For clear skies in which the atmosphere is considered optically thin, direct beam radiation can constitute 80 - 90% of the total radiation observed by a satellite. The more complex scattering terms can often be neglected, which leaves a relatively simple expression of satellite observed radiance in terms of G_λ, τ_λ, m, $r_{\lambda v}$, $r_{\lambda v}$ and γ. A straightforward application of proportion estimation for a two component system, i.e., soil and vegetation, would include equation (10) with four unknowns; m, $r_{\lambda v}$ $r_{\lambda s}$, and the term $G_\lambda \exp(-\tau_\lambda)/\pi$. Inclusion of shadow effects from a conifer forest (modeled as cones) would involve an additional unknown, γ.

The application of equations (10) or (11) to the determination of m depends on the data set being used and on the number of a priori assumptions one is willing to accept about other parameters, such as $r\lambda v$, $r\lambda s$, and $\tau\lambda$. The use of multispectral bands can help reduce the

number of unknowns, especially if reasonable assumptions are made regarding the relationship between a given parameter in different bands. The results of several variations of these models tested with field data are provided in a later section of this report.

Two Band Method

The ideal canopy cover algorithm would not only provide percent coverage of individual pixels, as well as several parameters such as vegetation and soil reflectivities, but would do so without the need for ground truth. The following procedure was investigated as a step toward achieving that goal.

It has been observed in a manner similar to previous authors (e.g., Kauth and Thomas, 1978), that MSS data plot in characteristic shapes in the two, three, or four-band space. For the MSS bands 4 and 2, with band 4 plotted along the ordinate and band 2 along the abscissa, the data typically fall in a triangular-like shape in the upper half plane with curved sides and a flat base and with sometimes a "tasseled cap". This has indeed been true for the Taos Study Area whether one plots the entire region (all types of vegetation) as shown in Exhibit 2, or segments of the region, as shown in Exhibit 3 for the valley area, and Exhibit 4 for the foothills region.

It can be shown using the direct beam equation that such characteristic triangular shapes can be explained in terms of the percent coverage of vegetation as well as the absolute values of the vegetation and soil reflectances. The starting point is the expression for direct beam, equation 10, written in terms of reflectances for MSS bands 2 and 4, or

$$r_2 = m(r_{2v} - r_{2s}) + r_{2s} \qquad (12)$$

$$r_4 = m(r_{4v} - r_{4s}) + r_{4s} \quad (13)$$

where

r_{2v}, r_{4v} = vegetation reflectance in MSS bands 2 and 4, respectively,

r_{2s}, r_{4s} = soil reflectance in MSS bands 2 and 4, respectively, and

r_2, r_4 = total observed reflectance of pixel in bands 2 and 4, respectively.

A simple triangular shape can be achieved by setting r_{2v}, and r_{4v} constant, and letting r_{2s} and r_{4s} vary over a range of values. A line representing m = 0, or "soil line" (or "background line") will form the base of the triangle stemming from the origin. Lines for values of $m > 0$ will plot above but parallel to the soil line. The value for m=1, or full coverage, will plot as a single point at the apex of the triangle. For instance, a simple triangle is illustrated in Exhibit 5 for the case of a landscape with a single vegetation species with constant reflectivity. That shape was drawn using $r_{2v} = 0.10$, $r_{4v} = 0.40$, and soil reflectivities falling in the intervals $0.08 \leq r_{2s} \leq 0.40$ and $0.10 \leq r_{4s} \leq 0.50$. The only constraint is that r_{2s}/r_{4s} remain approximately constant which is a reasonable assumption.

The effect of changing the reflectivity values is shown in Exhibit 6 (changes of vegetation reflectivity) and Exhibit 7 (changes in soil reflectivity). For instance, Exhibit 6 indicates that increasing r_{2v} will tend to flatten the triangular data space by moving the top of the triangle toward the soil line. An increase in r_{4v} will cause the opposite effect. A change in either r_{2v} or r_{4v} will have no effect on the soil line as one expects.

The simple model yielding a triangular shape can be extended to include the effects of varying vegetation reflectivity and shadows. For instance, by assuming that vegetation reflectivity is linearly related to percent cover, the triangular shape takes on curved sides as shown in Exhibit 8. The inclusion of shadows caused by conical figures will cause the triangle to take on a tasseled cap as shown in Exhibit 9. While other variations in plant parameters might cause similar effects, the above examples illustrate how the characteristic shape of the data space can be explained in terms of physical attributes of the components of the pixel. Application of the two-band model to field data is provided later in this report.

Empirical Estimators of Vegetation Parameters

Numerous vegetation indices have been proposed in recent years as qualitative indicators of green vegetation. The purpose has been to reduce the several multispectral bands to one value to estimate vegetation parameters such as biomass, leaf area index, or percent cover. Perry et al. (1984) summarize the many different vegetation indices and describe their relationship to each other. Three such indices are the normalized vegetation index, the perpendicular vegetation index, and the Kauth-Thomas Greenness index.

Normalized Vegetation Index

Of the many indices proposed, the normalized vegetation index (NVI) has evolved as a practical popular choice for use in regression with vegetation parameters. It is of the form

$$NVI = \frac{r_{IR} - r_{VIS}}{r_{IR} + r_{VIS}} \tag{14}$$

where r_{IR} and r_{VIS} represent the pixel reflectivity in the IR and visible ranges, respectively. Low NVI indicates low vegetation amount, whereas high NVI indicates either high vegetation amount or high productivity (Curran, 1980). Sellers (1985) discussed the functional relationship between the normalized VI and several vegetation parameters, including the leaf area index. Tucker et al. (1983) correlated the NVI (computed from NOAA's AVHRR data) to actual biomass obtained from field sampling in a semi-arid region of Senegal, West Africa. The effect of soil background on NVIs computed from hand-held or airborne radiometer data was investigated by Elvidge et al., 1985, and Huete et al., 1985.

Physical Basis. While the behavior of NVI can be qualitatively described in terms of chlorophyll absorption in the red region and scattering due to leaf area index in the near infrared, it can also be explained in terms of percent cover using the direct beam equation written in terms of reflectivities (12) and (13). Inserting (12) and (13) into (14) yields,

$$NVI = \frac{m[(r_{4v} - r_{4s}) - (r_{2v} - r_{2s})] + r_{4s} - r_{2s}}{m[(r_{4v} - r_{4s}) + (r_{2v} - r_{2s})] + r_{4s} + r_{2s}} \tag{15}$$

It is now noted that theoretically, the reflectance of any pixel composed of only one type of soil and vegetation must fall between the limits prescribed by the pure canopy and pure soil reflectivities shown in Exhibit 1. Using typical values for r_{4s}, r_{2s}, r_{4v} and r_{2v} as indicated, it is reasoned that the expression $(r_{4v} - r_{4s})$ is generally a positive value, whereas $(r_{2v} - r_{2s})$ is generally negative. As m increases,

the numerator becomes more positive, while the denominator decreases. Thus NVI should increase with increasing percent vegetation cover, as has been observed.

Perpendicular Vegetation Index

Richardson and Wiegard (1977) proposed the perpendicular vegetation index (PVI) as a measure of plant development. Application of this index first requires the establishment of a background soil line by linear regression of MSS bands 2 and 4 using bare soil pixels. The soil line is thus a straight line stemming from near the origin. The PVI is the perpendicular distance from the soil line to the actual data point which contains vegetation, and is defined,

$$PVI = [(r_{g2} - r_{p2})^2 + (r_{g4} - r_{p4})^2]^{1/2} \quad (16)$$

where

r_{g2}, r_{g4} = reflectances of soil background in bands 2 and 4, respectively, corresponding to the data point.

r_{p2}, r_{p4} = reflectances of data point in bands 2 and 4, respectively, perpendicular to r_{g2} and r_{g4} on the soil line.

Richardson et al. (1977) regressed PVI with percent cover of sorghum with a correlation coefficient of 0.57. Theis et al. (1984) studied the effect of vegetation and soil moisture on PVI. Rosenthal et al. (1985) recently used the PVI to investigate crop height and biomass.

Physical Basis. The behavior of the PVI can be readily demonstrated in terms of percent cover using the two-band method presented earlier, although the methods are slightly different. By setting r_{2v} and r_{4v} constant and letting r_{2s} and r_{4s} range from dark to bright values, a tri-

angular data space can be drawn. The base of the triangle, or soil line, stems from the origin and represents the condition m = 0. As m increases, the data space moves perpendicularly from the soil line. Thus, the PVI performs remarkably well in describing the physical shape of the data space when explained in terms of percent vegetation cover.

Kauth-Thomas Greenness Index

Kauth and Thomas (1926) applied Gram-Schmidt orthogonalization to the original four Landsat bands resulting in a new four-dimensional space termed "tasseled cap". The procedure, which is similar to principle components except in the order of calculations, essentially rotates the data so that most of the variability can be explained in terms of four indices; greenness (GI), brightness (BI), yellowness (YI), and nonsuch (NI). The first two of these indices are defined,

$$BI = 0.332\ DN1 + 0.603\ DN2 + 0.676DN3 + 0.263\ DN4 \quad (17)$$

$$GI = -0.283\ DN1 - 0.660\ DN2 + 0.577DN3 + 0.388\ DN4 \quad (18)$$

where DN1, DN2, DN3, and DN4 represent the digital counts of the three visible and one near infrared bands of the MSS scanner, respectively. A similar set of equations has been developed for the Thematic Mapper (Crist, 1983, Crist et al., 1984).

The Kauth-Thomas Transformation has been used by numerous investigators to model various crop parameters including crop development, moisture stress, yield and crop classification (Ezra et al., 1984). Huete et al. (1984, 1985) in a series of small scale experiments of wooden boxes filled with soil, showed high correlation of GI with percent cover. Musick (1984), however, using Landsat MSS data over New Mexico, was unable to achieve consistent differentiation between arid rangeland cover changes using GI.

Application of Canopy Cover Algorithms to Taos Study Area

Several different canopy algorithms described above have been tested at a preliminary level for a site located near Taos, New Mexico. The database consisted of Landsat MSS data, and 1:3000 aerial photographs, both supplied by the Bureau of Land Management. Details of the test site selection, and data acquisition and processing are provided in Jasinski and Eagleson (1986).

The Taos Study Area is outlined in Exhibit 10. The land includes a wide variation in surface relief, ranging from flat plains to rolling foothills, to detached high ridges. Elevation ranges from 6,000 to 10,000 feet. Vegetation tends to follow the topography. The lower flats are covered with blue grama and wheatgrass grasslands, and snakeweed, rabbitbrush and sagebrush shrublands. Pinyon-juniper woodlands are found in the rolling foothills. At the higher elevations, there is ponderosa pine, spruce, fir and aspen. Percent cover ranges from nearly 0 to 100 percent, with the majority of the area 40 to 60 percent covered. At least two trends in percent vegetation cover can be readily observed. They are, first, a decreased percent vegetation cover with decreasing altitude, and second, a less dense cover on south-facing slopes compared to north facing slopes at the same elevation.

Regression with Normalized Vegetation Index

Three variations of this approach were tested by regression with ground truth obtained from aerial photographs. A total of 116 pixels were used. The first variation involves using the normalized vegetation index with reflectivities as defined in equations (12) and (13). A second variation uses the normalized vegetation index defined in terms of actual integer DN values instead of reflectivities. The third approach

uses actual radiances. Details of these earlier studies were reported by Jasinski and Eagleson (1986). Only the results are provided in Table 1 below and shown on Exhibits 11, 12, and 13.

Table 1

Normalized Vegetation Index

versus Percent Cover

NVI Variation	m	R^2
$VI_r = \frac{r_4 - r_2}{r_4 + r_2}$	$m = 2.36\ VI_r + 6.68$	0.56
$VI_{DN} = \frac{2 \times DN_4 - DN_2}{2 \times DN_4 + DN_2}$	$m = 1.99\ VI_{DN} + 0.95$	0.61
$VI_R = \frac{R_4 - R_2}{R_4 + R_2} \times 100$	$m = 3.06\ VI_R - 111$	0.58

The results indicate that about 60% of the change in NVI can be explained in terms of percent vegetation cover, no matter which variation is used. The method is quick, requiring little analysis or computational time.

There are several limits to the use of NVI for estimating percent cover. First, the procedure needs to be calibrated with ground truth. Second, its accuracy is dependent on the vegetation and soil reflectivities in each band being relatively constant, and also limited to $r_{2s} > r_{2v}$ and $r_{4v} > r_{4s}$. For regions which are relatively uniform in vegetation type, however, the method provides good results of percent cover.

Regression Using Direct Beam Equation

Assuming that the landscape consists of only two cover types, soil and vegetation, equation (10) can be rewritten,

$$m = \frac{1}{(r_{\lambda v} - r_{\lambda s})} \left[\frac{L_{nr\lambda}}{\frac{G_\lambda}{\pi} \exp(-\tau_\lambda)} - r_{\lambda s} \right] \qquad (19)$$

For constant reflectivities, m is approximately linearly related to the observed radiance. With this in mind several linear regressions were carried out with m as the dependent variable and the observed radiances as dependent variables. The results are shown in Exhibits 14 and 15 and summarized in Table 2.

Table 2

Summary of Linear Regressions

Regression Equation	R^2
$m = 126 - 199R2$	0.53
$m = 377 - 138R4$	0.10
$m = 143 - 189R2/\cos\theta$	0.42
$m = 120 - 197\ R2 \cos\beta$	0.53
$m = 135 - 185\ R2 \cos\beta/\cos\theta$	0.44

where R2 and R4 are the observed radiances in MSS bands 2 and 4, respectively.

Two modifications to the above linear regressions were made. First, since G_λ is a function of the cosine of the zenith angle θ, equation (19) can be rewritten

$$m = \frac{1}{(r_{\lambda v} - r_{\lambda s})} \left[\frac{L_{nr\lambda}}{\frac{G'_\lambda \cos\theta}{\pi} \exp(-\tau_\lambda)} - r_{\lambda s} \right] \qquad (20)$$

Second, slight corrections to the observed radiance can be made in the case of non-horizontal surfaces. For surfaces with average slope β, the equation for m can be rewritten

$$m = \frac{1}{(r_{\lambda v} - r_{\lambda s})} \left[\frac{L_{nr\lambda} \cos\beta}{\frac{G'_{\lambda} \cos\theta}{\pi} \exp(-\tau_{\lambda})} - r_{\lambda s} \right] \qquad (21)$$

For the above two cases, ground slope and azimuth of individual pixels were measured from USGS 7.5-minute topographic maps. Zenith angle was computed using the following formula (Iqbal, 1983),

$$\begin{aligned} \text{Cos } \theta = {} & (\sin\phi \cos\beta - \cos\phi \sin\beta \cos\gamma) \sin\delta \\ & + (\cos\phi \cos\beta + \sin\phi \sin\beta \cos\gamma) \cos\delta \cos\omega \\ & + \cos\delta \sin\beta \sin\gamma \sin\omega \end{aligned} \qquad (22)$$

δ = solar declination

ω = hour angle

γ = surface azimuth angle

β = average slope of pixel

Solar declination and hour angle were estimated from knowing time of Landsat overpass.

The results of the linear regressions including the new parameters are surprisingly poor, as indicated on Exhibits 16, 17 and 18, and on Table 2. In no case is the correlation improved. Part of the explanation for the poor correlation may simply be due to the bidirectional reflection characteristics of the soil. A likely explanation may also simply be the inaccuracies introduced by measuring small distances off the topographic maps. At the 1:24000 scale, pixels are less than 0.2 cm^2

in area and small inaccuracies in measurement or pixel registration can cause serious error in the regression analysis.

Use of the direct beam equation for estimating m has required a set of ground truth. Having the ground truth, it is theoretically possible to estimate the quantities $\pi/[(r_{\lambda v} - r_{\lambda s})G_{\lambda t} \exp(-\tau_\lambda)]$ and $r_{\lambda s}/(r_{\lambda v} - r_{\lambda s})$ from the coefficients of the linear regression. If functional relationships can be established between the individual parameters for each band (e.g., $r_{2\lambda} = f(r_{4\lambda})$) it is also possible, at least in theory, to calculate all the reflectivity values $r_{2v}, r_{4v}, r_{2s}, r_{4s}$ as well as the quantities $G_{2t} \exp(-\tau_2)$ and $G_{4t} \exp(-\tau_4)$ using data from bands 2 and 4.

Regression with Kauth-Thomas Indices

The Kauth-Thomas greenness and brightness indices were computed and then regressed with actual percent cover obtained from the aerial photographs. The results which are somewhat poorer than anticipated, are shown in Table 3. They indicate, contrary to expectation, that brightness appears to explain more of the variation in m than greenness.

Table 3

Kauth-Thomas Indices

Index	R^2
Greenness, GU	0.24
Brightness, BI	0.39

The regression analyses yielded,

$$m = 10.47 + 0.14\ GI$$

$$m = 82.82 - 0.48\ BI$$

Multiple Linear Regression

Multiple linear regressions were carried out with the same data set as in previous cases with percent cover as the dependent variable and the MSS band observations as independent variables. The two cases examined were m vs. DN1 and DN2, and m vs. DN1, DN2, DN3 and DN4. Once regression coefficients were obtained, theoretical percent cover obtained from the multiple linear regression analysis was regressed with actual percent cover in order to compare correlation coefficients with other methods. The results for the second case are shown on Exhibit 19 (for regression with four bands) and summarized on Table 4.

Table 4

Results of Multiple Linear Regression

Regression Equation	R^2
$m = -2.25\ DN2 + 0.70\ DN4 + 74.97$	0.53
$m = -2.07\ DN1 - 0.62\ DN2 + 0.20\ DN3 + 0.63\ DN4 + 72.25$	0.58

As expected, there is negative correlation with the visible bands and positive with the near infrared. It is also noted that the addition of bands 1 and 3 only contributes an increase of 0.05 in R^2.

Two-band Model

The two-band model as presented was applied to the foothills segment of the scene where the type of vegetation was believed to be relatively homogeneous. Two cases were investigated, those assuming constant and variable (with m) vegetation reflectivities.

Application of the model consists of the following steps:

1) All data points within the segment are plotted.

2) Envelope lines are drawn along the three sides of the triangular data space. The soil line is drawn as a straight line emanating from the origin. (For the assumption of no shadows and constant vegetation reflectivities, all sides of the triangle must be drawn straight.)

3) Along the soil line, m is assumed equal to zero. Likewise, at the top of the triangle, m is assumed equal to one.

4) The calculation of m for any data point within the triangle depends on the assumptions made. For constant vegetation reflectivity, m is assumed linearly related to the distance between the top and base of the triangle. For example, for a point exactly halfway between the top and the base, m is assumed equal to 50% cover. For the case of vegetation reflectivity linearly related to percent cover, m is estimated on the basis of the shape of the envelope curves, which can be approximated as second order polynomials in m.

The graphical results of the analyses applied to the Taos data are shown in Exhibits 20 through 23. Exhibits 20 and 21 include identical plots of all the data in the particular segment chosen (2250 pixels). It is noted that the data space takes on a classical triangular shape. Exhibit 20 also includes straight line envelope curves under the assumption of constant vegetation reflectivity. Exhibit 21 includes curved envelope lines under the assumption that vegetation reflectivity is linearly related to m. Percent cover for each case was then estimated according to the procedure outlined above.

Exhibits 22 and 23 include only the data points with ground truth. In order to test the validity of the method, it was necessary to locate the data points with ground truth within the triangle and compare the

actual percent cover, m, to that estimated graphically, m_g. The R^2 values resulting from the regression of m_g with m are shown in Table 5.

Table 5

Results of Two-Band Models

Two-Band Model Version	R^2
1) Constant Vegetation Reflectivity	0.34
2) Variable r_v	0.30

Conclusions

There are several important conclusions which can be drawn from this past year's work. In general, the results have established the feasibility of estimating percent canopy cover using either physically-based or empirical models. The most successful empirical model for the Taos Study Area was the normalized vegetation index, which explained about 60 percent of its variability in terms of m. About 50 percent of the variability of the direct beam equation for the visible band could be explained in terms of m using constant canopy and soil reflectivities. For the near infrared band, only 10 percent of the variability could be explained for the same conditions. The two-band model was able to explain about 35 percent of its variability in terms of m.

While the use of NVI produced the best correlation, the results have depended on the availability of ground truth. Its application to other natural regions is therefore unknown. That is also true for the physically-based models which use only one band, even with the incorporation of slope and shadows.

It has also been shown that the characteristic triangular shape of the two-band data space (MSS bands 2 and 4) can be explained in terms of percent canopy cover, although other vegetation parameters, such as leaf area and canopy reflectance, can also contribute to such shapes. A simple version assuming constant canopy reflectance provided encouraging results when applied to the Taos Study Area.

The major advantage of the two-band model is in its ability to estimate canopy cover without ground truth. It uses the entire data set and provides the possibility of estimating other vegetation parameters by careful incorporation of the limits of the data space into the analysis.

The simple version presented can be extended relatively easily to include topography, shadows, leaf area, and variability (randomness) in canopy reflectance (see Future Work).

There is always some uncertainty regarding the error introduced through the data themselves. That includes inaccuracies in the estimation of percent cover from the aerial photographs, errors in registration of both the Landsat scene as well as the aerial photographs, anomalies in the Landsat data, errors introduced through data filtering, and finally, in the conversion of DN values to actual radiometric quantities. There appears to be no easy way to estimate the magnitude of each of these effects. Several of the more successful procedures should be applied to an entirely new data set outside the Taos Study Area.

Future Work

There are at least two research areas which have not yet been exploited in the development of a working canopy cover algorithm using Landsat data. The first involves an investigation of the random distribution of the radiances when plotted in two-, three-, or four-band space. The second involves the incorporation of additional surface parameters into the canopy cover algorithm. Future work will try to combine both these areas in order to extend the two-band procedure introduced this past year. Further details are described below together with an outline of the proposed mathematical formulation.

While the two-band method incorporates the limits of the data space in determining m, it does not take full advantage of the distribution of the radiances within the data space. A hypothetical example is shown in Exhibit 24. By treating the observed radiances of the visible and near infrared bands (R2 ,R4) as random fields, a joint probability distribution can be obtained. Most of the information of the segment is located within the interior of the data space, and not along the limits which envelope the data. Up to now, the simple two-band model has incorporated only information about the limits in a deterministic sense. By incorporating randomness into the formulation, information contained in the entire data set can be used. The above approach can be easily extended to include the randomness of three- and four-band data spaces.

The second area which needs further research is the incorporation of additional surface features into the canopy cover algorithm. Much of the Taos Study Area is located in rolling foothills. It is obvious from the aerial photographs that vegetation type and percent cover is a function of the elevation, slope and azimuth of the land. The combined effect of

all those features is qualitatively seen in the Landsat images of individual bands. It has been shown earlier in this report that such parameters as shadows, ground slope and azimuth, leaf area index, and species can be incorporated into the physical model. Several of those features which were examined individually now need to be incorporated into one model. A specific problem which needs to be worked out is the effect of shadows for sloping surfaces on observed reflectivity.

The following mathematical formulation is intended to incorporate the effects of both randomness and additional surface parameters into a physically based canopy cover algorithm. The formulation is presented for the case of two bands. The starting point is the direct beam equation which can be written very generally in terms of reflectances for the visible (MSS band 2) and near infrared (MSS band 4) wavelengths,

$$r_2(m,\rho,L_2,\beta,\theta,s,u,w) = m\, r_{2v}(\rho,L_2,\beta,\theta,s,u) + (1-m) r_{2s}(\beta,\theta,n,w) \qquad (23)$$

$$r_4(m,\rho,L_4,\beta,\theta,s,u,w) = m\, r_{4v}(\rho,L_4,\beta,\theta,s,u) + (1-m) r_{4s}(\beta,\theta,n,w) \qquad (24)$$

where

m = percent vegetation cover

ρ = percent shadow parameter

L_2, L_4 = leaf area indices for bands 2 and 4, respectively

β = ground slope

θ = zenith angle, which includes effects of ground slope, ground azimuth, (altitude, hour angle, etc.)

s = vegetation species

n = soil moisture

u = a general parameter including factors other than those mentioned above causing variability in canopy reflectance, for example, stress, disease, etc.

w = a general parameter including factors other than those listed above causing soil reflectance variability, including organic content, grain size and distribution, mineral content, ... etc.

Written in the above form, all the variability in r_2 and r_4 is attributed to the variability in r_{2v} and r_{4v}. For example, since it has been demonstrated earlier that up to 60 percent of the variability in r_2 can be explained by m, it follows that the balance or 40 percent is due to $r_{2v}(\rho, L_2, \beta, \theta, s, u)$ and $r_{2s}(\beta, \theta, r, w)$ variability.

The next step is to try to remove some of that variability in r_{2v} and r_{2s} by incorporating the effects of additional parameters, for instance, slope and zenith angle. Introducing a new function, $g(\beta,\theta)$ to account for those effects, it can be shown that for flat surfaces (not necessarily horizontal),

$$g(\beta,\theta) = \cos\theta/\cos\beta$$

where $\cos\theta$ is given by equation (22). Therefore,

$$r_2 = g(\beta,\theta)[m\ r'_{2v}(\rho,L_2,s,u) + (1-m)r'_{2s}\ (n,w)] \tag{26}$$

$$r_4 = g(\beta,\theta)[m\ r'_{4v}(\rho,L_4,s,u) + (1-m)r'_{4s}\ (r,w) \tag{27}$$

where $$r'_{2v} = r_{2v}/g(\beta,\theta) \tag{28}$$

$$r'_{2s} = r_{2s}/g(\beta,\theta) \tag{29}$$

$$r'_{4v} = r_{4v}/g(\beta,\theta) \tag{30}$$

$$r'_{4s} = r_{rs}/g(\beta,\theta) \tag{31}$$

Similarly, variability due to shadows can be removed from r'_{2v} and r'_{4v} using various geometric models indicated earlier. Let $h(\rho)$ represent the effect of shadows manifested by a geometric model on a sloping bed. The variable ρ is a function of geometric shape (i.e., cone, cylinder) as well as slope, azimuth and zenith angle. The reflectances can be rewritten

$$r_2 = g(\beta,\theta)[m\ h(\rho)\ r''_{2v}\ (L_2 s,u) + (1-m)\ r'_{2s}(n,w)] \tag{32}$$

$$r_4 = g(\beta,\theta)[m\ h(\rho)\ r''_{4v}\ (L_4 s,u) + (1-m)\ r'_{4s}(n,w)] \tag{33}$$

where

$$r''_{2v} = r_{2v}/[g(\beta,\theta)\ h(\rho)]$$
$$r''_{4v} = r_{4v}/[g(\beta,\theta)\ h(\rho)] \tag{34}$$

In theory, one can continue developing functions f(L), j(s) and k(n) to remove more and more of the variability from r_{2v}, r_{4v}, r_{2s}, and r_{4s}. At each stage, however, additional unknowns are introduced into the formulation, each associated with more ground truth. Since the intention is to develop a model without the need for ground truth, it is reasonable to stop at this point where no field data are required and use equations (32) and (33) to estimate m in conjunction with the available information. Let us first summarize the data and the major assumptions.

The data include r_2 and r_4 obtained from the Landsat digital counts. It is assumed that the atmosphere is optically thin, thereby neglecting the scattering terms in the atmospheric radiative transfer equation. The parameters β and θ and hence $g(\beta,\theta)$ can be estimated from knowing time of Landsat overpass and from examination of USGS topographic maps.

The function $h(\rho)$ can be obtained analytically and requires additional reasonable assumptions. Those include the shape of the canopy (i.e., cones) and the spatial distribution of trees. For natural conifer forests, a poisson distribution has often been assumed (Matern, 1960, Strahler et al., 1981, Li et al., 1985).

The unknowns in equations (32) and (33) are thus m, r''_{2v}, r'_{2s}, r''_{4v}, and r''_{4s}. Making further the assumption

$$r''_{2v} = f(\lambda_2)\ A(s,u) \tag{35}$$

$$r''_{4v} = f(\lambda_4)\ A(s,u) \tag{36}$$

$$r'_{2s} = g(\lambda_2)\ B(n,w) \tag{37}$$

$$r'_{4s} = g(\lambda_4)\ B(n,w) \tag{38}$$

where $f(\lambda)$ and $g(\lambda)$ are normalized reflectivity functions ranging from zero to one, equations (32) and (33) become

$$r_2 = g(\beta,\theta)[m\ h(\rho)\ f(\lambda_2)\ A(s,u) + (1-m)\ g(\lambda_2)\ B(n,w)] \tag{39}$$

$$r_4 = g(\beta,\theta)[m\ h(\rho)\ f(\lambda_4)\ A(s,u) + (1-m)\ g(\lambda_4)\ B(n,w)] \tag{40}$$

There are now three unknowns, m, A(s,u) and B(n,w), associated with equations (39) and (40). While the problem still requires one more equation, it has been greatly simplified by making only a few reasonable assumptions and without ground truth, except for topographic data.

There are several approaches one can take to solve equations (39) and (40). The first is to obtain a derived probability distribution of m of the form

$$m = m[r_2,\ r_4,\ A(s,w),\ B(n,w)] \tag{41}$$

This can be done numerically. The random functions A(s,w) and B(n,w) might be obtained by conditionalizing on r_2 and r_4.

A second approach is to introduce a third equation r_1 or r_3 using either of the two remaining Landsat MSS bands, although problems of independence between bands 1 and 2 or 3 and 4 might arise.

A third approach is to simply assume a priori that the data falling on the lower base of the data space triangle reflect background. This leads to a direct calculation of the probability density function for B(n,w), by conditionalizing along that background line. Once determined, one can compute by means of equations (39) and (40), the two remaining unknowns, A(s,u) and m.

It is not known which of the above three approaches work best for obtaining the desired third equation. The third approach, assuming a soil line, appears the most straightforward. It is also consistent with other research which attempts to use the soil line as an important parameter in vegetation modeling. Future work will examine and evaluate each of those alternatives.

REFERENCES

Amis, M.L., R.K. Lennington, M.V. Martin, W.G. McGuire, and S.S. Shen (1981), "Evaluation of Large Area Crop Estimation Techniques," Proceedings of the Fifteenth International Symposium on Remote Sensing of Environment, Ann Arbor, Michigan, May, 1981, pp. 1047-1056.

Chen, J. (1985), "Kubelka-Munk Equations in vector-matrix forms and the solution for bidirectional vegetative canopy reflectance," Applied Optics, Vol. 24, No. 3, pp. 376-382.

Chhikara, R.S. (1984), "Effect of Mixed (Boundary) Pixels on Crop Proportion Estimation," Remote Sensing of Environment, Vol. 14, pp. 207-218.

Colwell, J.E. (1974), "Vegetation Canopy Reflectance," Remote Sensing of Environment, Vol. 3, pp. 175-183.

Crist, E.P. (1983), "The Thematic Mapper Tasseled Cap--A Preliminary Formulation," in Machine Processing of Remotely Sensed Data Symposium, pp. 357-364.

Crist, E.P. and R.C. Cicone (1984), "A Physically-Based Transformation of Thematic Mapper Data," IEEE Transactions on Geoscience and Remote Sensing, Vol. GE-22, No. 3, pp. 256-263.

Curran, P. (1980), "Multispectral Photographic Remote Sensing of Vegetation Amount and Productivity," Proceedings of the Fourteenth International Symposium on Remote Sensing of Environment, Ann Arbor, Michigan, pp. 623-637.

Dave, J.V. (1980), "Effect of Atmospheric Conditions on Remote Sensing of a Surface Nonhomogeneity," Photogrammetric Engineering and Remote Sensing, Vol. 46, No.9, September 1980, pp. 1173-1180.

Dickinson, R.E. (1983), "Land Surface Processes and Climate-Surface Albedos and Energy Balance," in Advances on Geophysics, Vol. 25, pp. 305-353.

Dozier, J. (1981), "A Method for Satellite Identification of Surface Temperature Fields of Subpixel Resolution," Remote Sensing of Environment, Vol. 11, pp. 221-229.

Eagleson, P.S. (1982), "Ecological Optimality in Water-Limited Natural Soil-Vegetation Systems 1. Theory and Hypothesis," Water Resources Research, Vol. 18, No. 2, pp. 325-340.

Eagleson, P.S. and T.E. Tellers (1982), "Ecological Optimality in Water-Limited Natural Soil Vegetation Systems 2. Tests and Applications," Water Resources Research, Vol. 18, No. 2, pp. 341-354.

Elvidge, C.D., and R.J.P. Lyon (1985), "Influence of Rock-Soil Spectral Variation on the Assessment of Green Biomass," Remote Sensing of Environment, Vol. 17, p. 265-279.

Estes, J.E., E.J. Hajic, and L.R. Tinney (1983), "Fundamentals of Image Analysis: An Analysis of Visible and Thermal Infrared Data," in Manual of Remote Sensing, American Society of Photogrammetry, Chapter 24, pp. 987-1124

Ezra, C.E., L.R. Tinney and R.D. Jackson (1984), "Effect of Soil Background on Vegetation Discrimination Using Landsat Data," Remote Sensing of Environment, Vol. 16, pp. 233-242.

Gates, D.M. (1970), Remote Sensing, National Academy of Sciences, p. 224.

Gerstl, A.W. and A. Zardecki (1985), "Coupled Atmosphere/Canopy Model for Remote Sensing of Plant Reflectance Features," Applied Optics, Vol. 24, No. 1, pp. 94-103.

Goel, N.S. and D.E. Strebel (1983), "Inversion of Canopy Reflectance Models for Estimating Agronomic Variables. I. Problem Definition and Initial Results Using the Suits Model," Remote Sensing of Environment, Vol. 13, pp. 487-507.

Goel, N.S., D.E. Strebel, and R.L. Thompson (1984a), "Inversion of Vegetation Canopy Reflectance Models for Estimating Agronomic Variables. II. Use of Angle Transforms and Error Analysis as Illustrated by Suits' Model," Remote Sensing of Environment, Vol. 14, pp. 77-111.

Goel, N.S. and R.L. Thompson (1984b), "Inversion of Vegetation Canopy Reflectance Models for Estimating Agronomic Variables. III. Estimation Using Only Canopy Reflectance Data as Illustrated by the Suits Model," Remote Sensing of Environment, Vol. 15, pp. 223-236.

Goel, N.S., and R.L. Thompson (1984c), "Inversion of Vegetation Canopy Reflectance Models for Estimating Agronomic Variables. IV. Total Inversion of the SAIL Model," Remote Sensing of Environment, Vol 15, pp. 237-253.

Goel, N.S. and R.L. Thompson (1984d), "Inversion of Vegetation Canopy Reflectance Models for Estimating Agronomic Variables. V. Estimation of Leaf Area Index and Average Leaf Angle Using Measured Canopy Reflectances," Remote Sensing of Environment, Vol. 16, pp. 69-85.

Horwitz, H.M., R.F. Nalepka, P.D. Hyde, and J.P. Morgenstern (1971), "Estimating the Proportions of Objects within a Single Resolution Element of a Multispectral Scanner," Proceedings of the 6th International Symposium on Remote Sensing of Environment, Willow Run Labs, The University of Michigan, Ann Arbor, pp. 1307-1320.

Huete, A.R., R.D. Jackson and D.F. Post (1985), "Spectral Response of a Plant Canopy with Different Soil Backgrounds," Remote Sensing of Environment, Vol. 17, pp. 37-53.

Huete, A.R., D.F. Post, and R.D. Jackson (1984), "Soil Spectral Effects on 4-Space Vegetation Discrimination," Remote Sensing of Environment, Vol. 15, pp. 155-165.

Iqbal, M. (1983), An Introduction to Solar Radiation, Academic Press.

Jasinski, M.F. and P.S. Eagleson (1986), "Feasibility of Using Landsat Images of Vegetation Cover to Estimate Effective Hydraulic Properties of Soils," Annual Technical Report on NAG 5-510.

Lang, A.R.G., X. Yuegin and J.M. Horman (1985), "Crop Structure and the Penetration of Direct Sunlight," Agriculture and Forest Meteorology, Vol. 35, pp. 83-101.

Kondratyev, K.Y.A. (1969), Radiation in the Atmosphere, Academic Press.

Lennington, R.K., C.T. Sorenson, and R.P. Heydon (1984), "A Mixture Model Approach for Estimating Crop Areas from Landsat Data," Remote Sensing of Environment, Vol. 14, pp. 197-206.

Li, X., and A.H. Strahler (1985), "Geometric-Optical Modeling of a Conifer Forest Canopy," IEEE Transactions on Geoscience and Remote Sensing, Vol. GE-23, No. 5, pp. 705-721.

McCloy, K.R. (1980), "The Response Characteristics of Vegetation in Landsat MSS Digital Data," Remote Sensing of Environment, Vol. 10, pp. 185-190.

Meador, W.E., and W.R. Weaver (1980), "Two-Stream Approximations to Radiative Transfer in Planetary Atmospheres: A Unified Description of Existing Methods and a New Improvement," Journal of Atmospheric Sciences, Vol. 37, March 1980, pp. 630-643.

Monsi, M., and T. Saeki (1953), "Über den Lichtfaktor in den Pflanzengesellschaften und seine Bedeutung für die Stoffproduktion," Jpn. J. Bot., 14(1), pp. 22-52,

Musick, H.B., "Assessment of Landsat Multispectral Scanner Spectral Indices for Monitoring Arid Rangeland," IEEE Transactions on Geoscience and Remote Sensing, Vol. GE-22, No. 6, pp. 512-519.

Myers, V.I. (1983), "Remote Sensing Applications in Agriculture," in Manual of Remote Sensing, American Society of Photogrammetry, Chapter 33, pp. 2111-2228.

Nalepka, R.F., H.M. Horwitz, and P.D. Hyde (1972), "Estimating Proportions of Objects from Multispectral Data," Technical Report No. 31650-73-T, Willow Run Labs, The University of Michigan, Ann Arbor.

Otterman, J. (1978), "Single-Scattering Solution for Radiative Transfer through a Turbid Atmosphere," Applied Optics, Vol. 17, No. 21, 1 November 1978, pp. 3431-3438.

Otterman, J., and R.S. Fraser (1979), "Adjacency Effects on Imaging by Surface Reflection and Atmosheric Scattering: Cross Radiance to Zenith," Applied Optics, Vol. 18, No. 16, 15 August 1979, pp. 2852-2859.

Otterman, J., S. Ungar, Y. Kaufman, and M. Podolak (1980), "Atmospheric Effects on Radiometric Imaging from Satellites under Low Optical Thickness Conditions," Remote Sensing of Environment, Vol. 9, pp. 115-129.

Otterman, J. (1981), "Reflection from Soil with Sparse Vegetation", Advances in Space Research, Vol. 1, pp. 115-119.

Otterman, J. (1984), "Albedo of a Forest Modeled as a Plane with Dense Protrusions," Journal of Climate and Applied Meteorology, Vol. 23, February, pp. 297-307.

Otterman, J. (1981), and G. H. Weiss (1984), "Reflection from a field of randomly located vertical protrusions," Applied Optics, Vol. 23, No. 12, pp. 1931-1936.

Perry, C.R. Jr., and L.F. Lautenschlager (1984), "Functional Equivalence of Spectral Vegetation Indices," Remote Sensing of Environment, Vol. 14, pp. 169-182.

Reyna, E., and G.D. Badhwar (1985), "Inclusion of Specular Reflectance in Vegetative Canopy Models," IEEE Transactions on Geoscience and Remote Sensing, Vol. GE-23, No. 5, pp. 731-736.

Richardson, A.J. and C.L. Wiegand (1977), "Distinguishing Vegetation from Soil Background Information," Photogrammetric Engineering and Remote Sensing, Vol. 43, No. 12, pp. 1541-1552.

Robinove, C.J. (1981), "The Logic of Multispectral Classification and Mapping of Land," Remote Sensing of Environment, Vol. 11, pp. 231-244.

Rosenberg, N.H., B.L. Blad, and S.B. Verma (1983), Microclimate, The Biological Environment. 2nd Edition, Wiley-Interscience, 1983.

Rosenthal, W.D., B.J. Blanchard, and A.J. Blanchard (1985), "Visible/Infrared/Microwave Agriculture Classification, Biomass, and Plant Height Algorithms," IEEE Transactions on Geoscience and RemoteSensing, Vol. GE-23, No. 2, pp. 84-90.

Ross, J. (1981), The Radiation Regime and Architecture of Plant Stands, Dr. W. Junk, Publishers, The Hague.

Sellers, P.J. (1985), "Canopy Reflectance, Photosynthesis and Transpiration," Draft Report, NASA/Goddard Space Flight Center, Hydrological Sciences Branch, Greenbelt, Maryland.

Simmer, C., and S.A.W. Gerstl (1985), "Remote Sensing of Angular Characteristics of Canopy Reflectances," IEEE Transactions on Geoscience and Remote Sensing, Vol. GE-23, No. 5, pp. 648-658.

Smith, J.A. (1983), "Matter-Energy Interaction in the Optical Region," in Manual of Remote Sensing, American Society of Photogrammetry, Chapter 3, pp. 61-113.

Strahler, A.H., and Li Xiaowen (1981), "An Invertible Coniferous Forest Canopy Reflectance Model," Proceedings of Fifteenth International Symposium on Remote Sensing of Environment, Ann Arbor, MI, pp. 1237-1244.

Strebel, D.E., H.S. Goel, and K.J. Ranson (1985), "Two-Dimensional Leaf Orientation Distributions," IEEE Transactions on Geoscience and Remote Sensing, Vol. GE-23, No. 5, pp. 640-647.

Suits, G.H. (1972), "Calculation of the Directional Reflectance of a Vegetation Canopy," Remote Sensing of Environment, Vol. 2, pp. 117-125.

Theis, S.W., B.J. Blanchard, and R.W. Newton (1984), "Utilization of Vegetation Indices to Improve Soil Moisture Estimates Over Agricultural Lands," IEEE Transactions on Geoscience and Remote Sensing, Vol. GE-22, No. 6, pp. 490-495.

Tucker, C.J., and L.D. Miller (1977), "Soil Spectra Contributions to Grass Canopy Spectral Reflectance," Photogrammetric Engineering and Remote Sensing, Vol. 43, No. 6, p. 721-726.

Tucker, C.J. (1980), "A Spectral Method for Determining the Percentage of Green Herbage Material in Clipped Samples," Remote Sensing of Environment, Vol. 9, pp. 175-181.

Tucker, C.J., C. Vanpraet, E. Boerwinkel, and A. Gaston (1983), "Satellite Remote Sensing of Total Dry Matter Production in the Senegalese Sahel," Remote Sensing of Environment, Vol. 14, pp. 461-474.

Ungar, S.G., and E. Bryant (1981), "Fanning: A Classification Algorithm for Mixture Landscapes Applied to Landsat Data of Maine Forests," Proceedings of the Fifteenth International Symposium on Remote Sensing of Environment, Ann Arbor, Michigan, May 1981, pp. 113-120.

Vanderbilt, V.C. and L. Grant (1985), "Plant Canopy Specular Reflect ance Model," IEEE Transactions on Geoscience and Remote Sensing, Vol. GE-23, No. 5, pp. 722-730.

Verhoef, W. and N.J.J. Bunnik (1981), "Influence of Crop Geometry on multispectral reflectance determined by use of canopy reflectance models," Proceedings of the International Colloquium on Signatures of Remotely Sensed Objects", Avignon, pp. 273-290.

Walthall, C.L., J.M. Norman, J.M. Welles, G. Campbell, and B.L. Blad (1983), "Simple equation to approximate the bidirectional reflectance from vegetative canopies and bare soil surfaces," Applied Optics, Vol. 24, No. 3, pp. 383-387.

Work, E.A. (1974), "Application of the Earth Resources Technology Satellite for Monitoring the Breeding Habitat of Migratory Waterfowl in the Glaciated Prairies," Master of Science Thesis, University of Michigan.

Work, E.A. (1983), "Taos Resource Area Remote Sensing Project," Final Report, Bureau of Land Management, Branch of Scientific Systems Applications, Denver, Colorado.

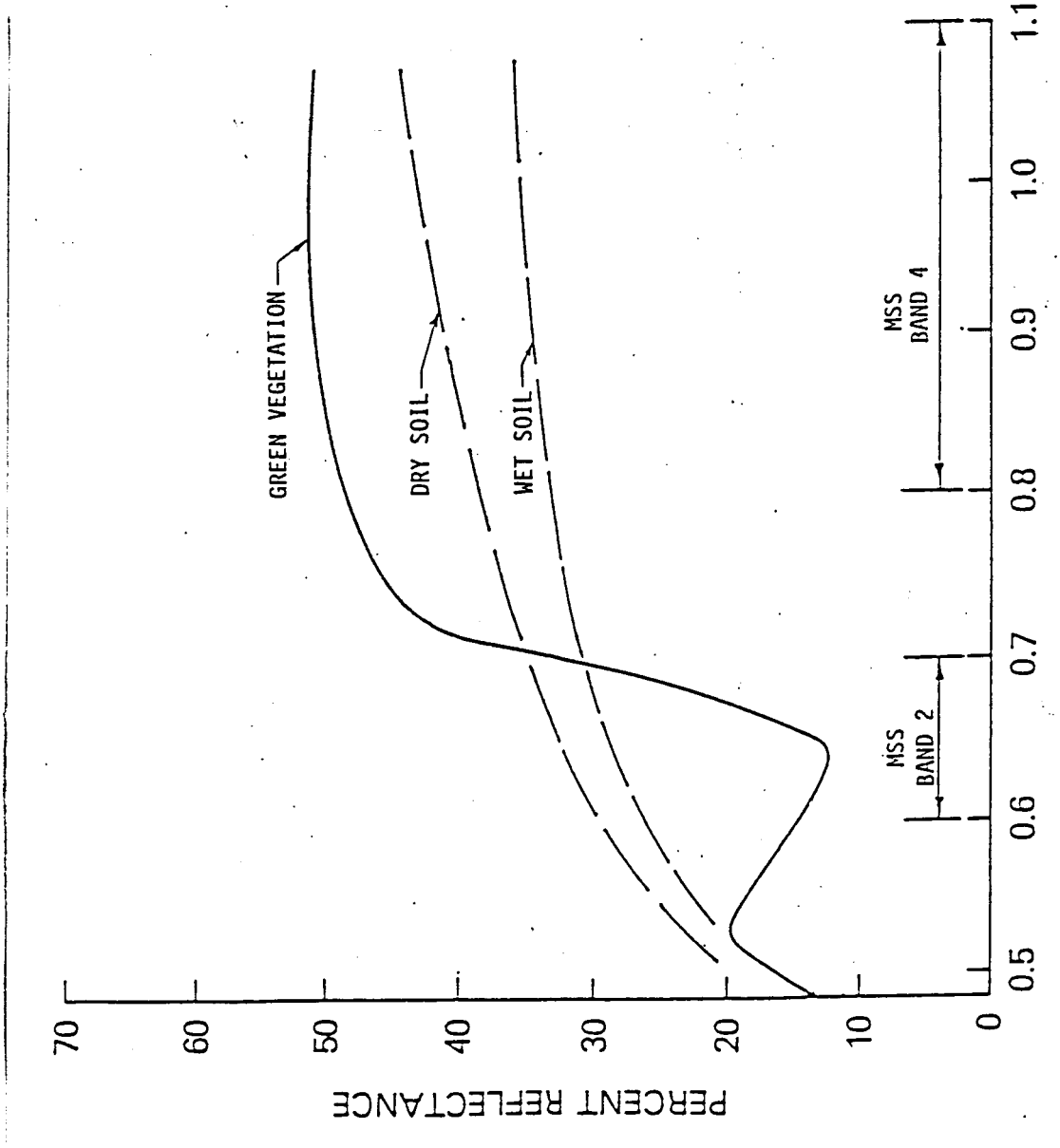

Typical Vegetation and Soil Reflectance Curves

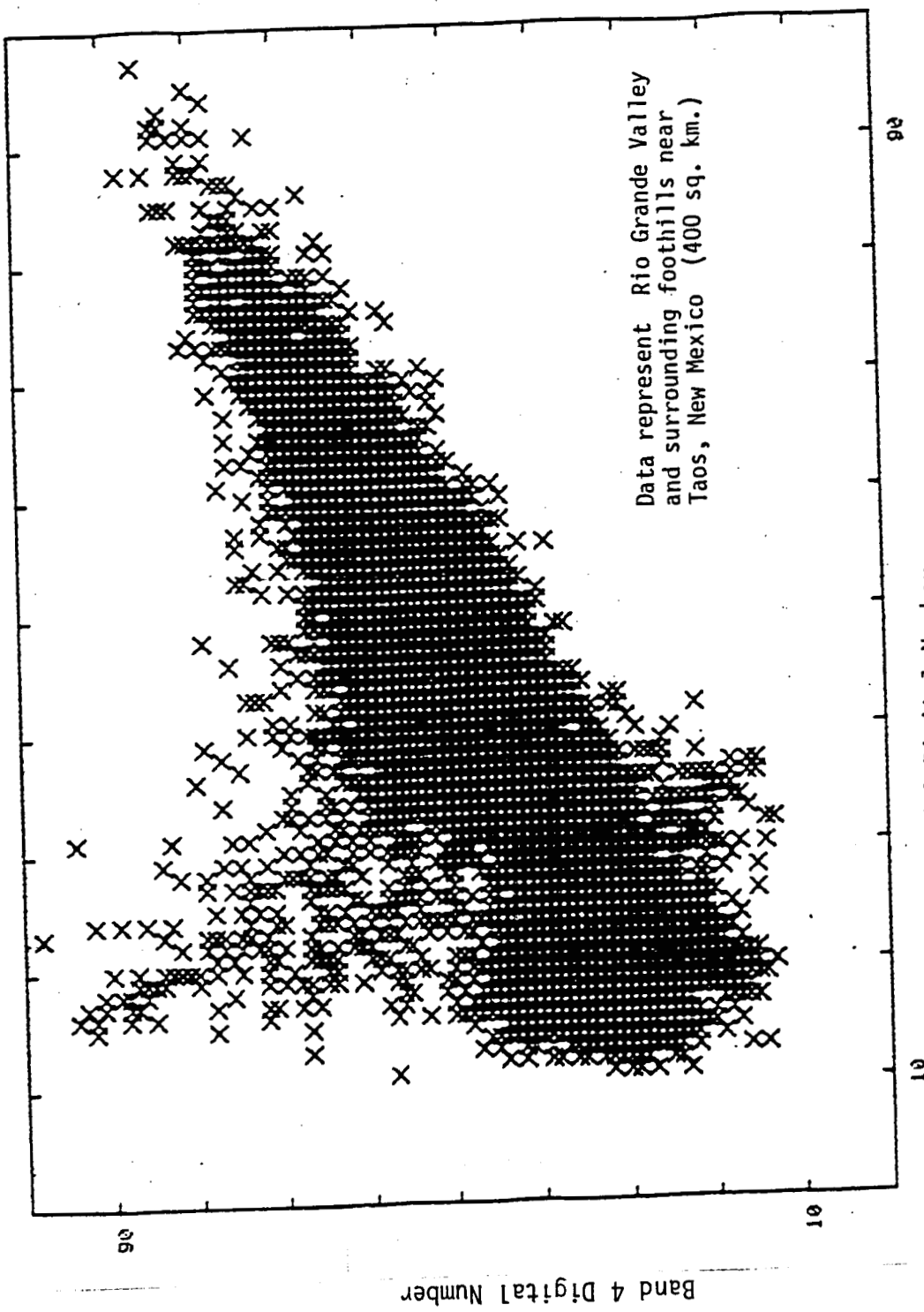

Data Plot of MSS Band 4 vs. MSS Band 2
Entire Taos Study Area (40,000 pixels)

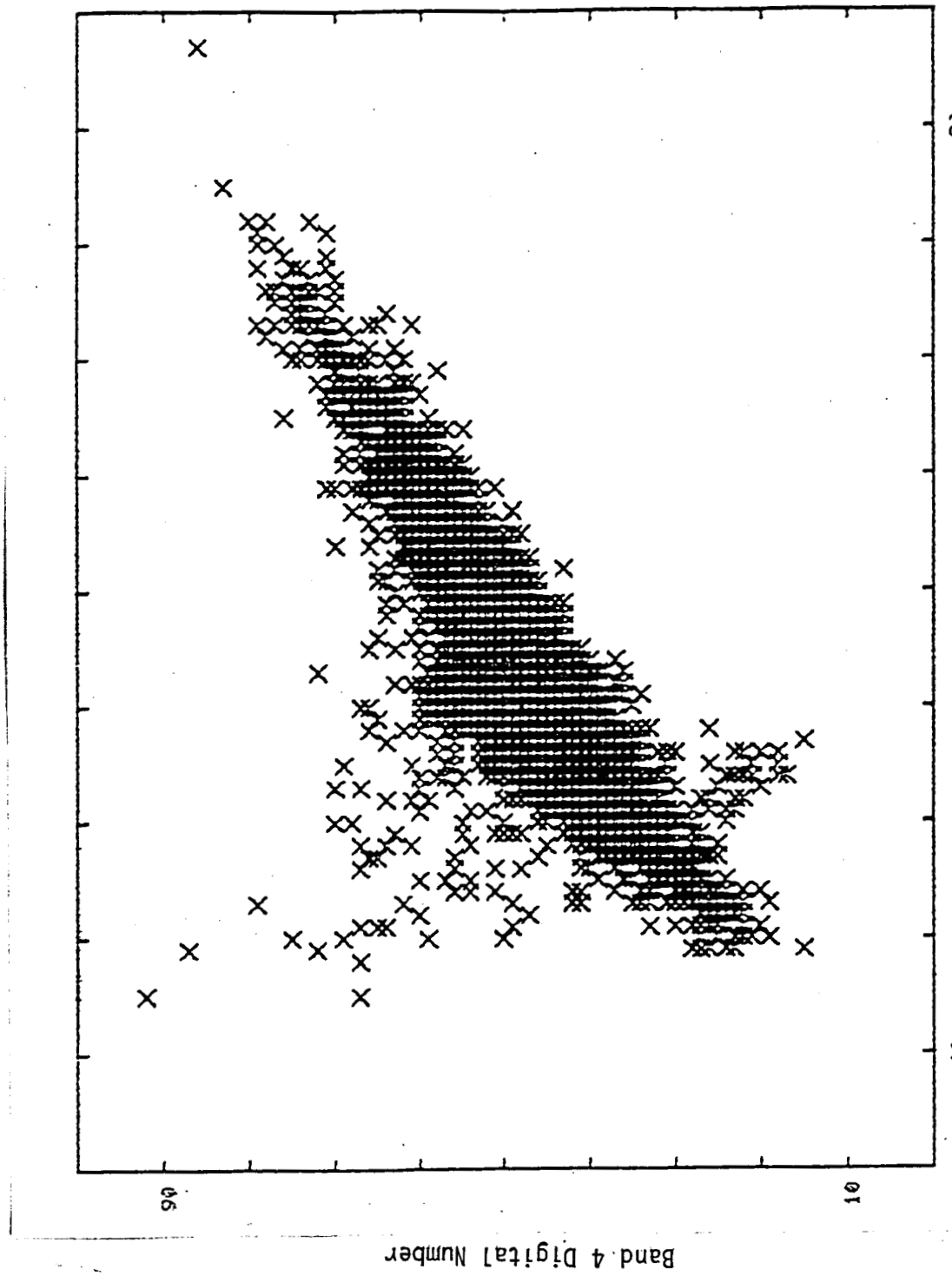

Data Plot of MSS Band 4 vs. MSS Band 2
Segment of Valley Region of Taos Study Area (8,000 pixels)

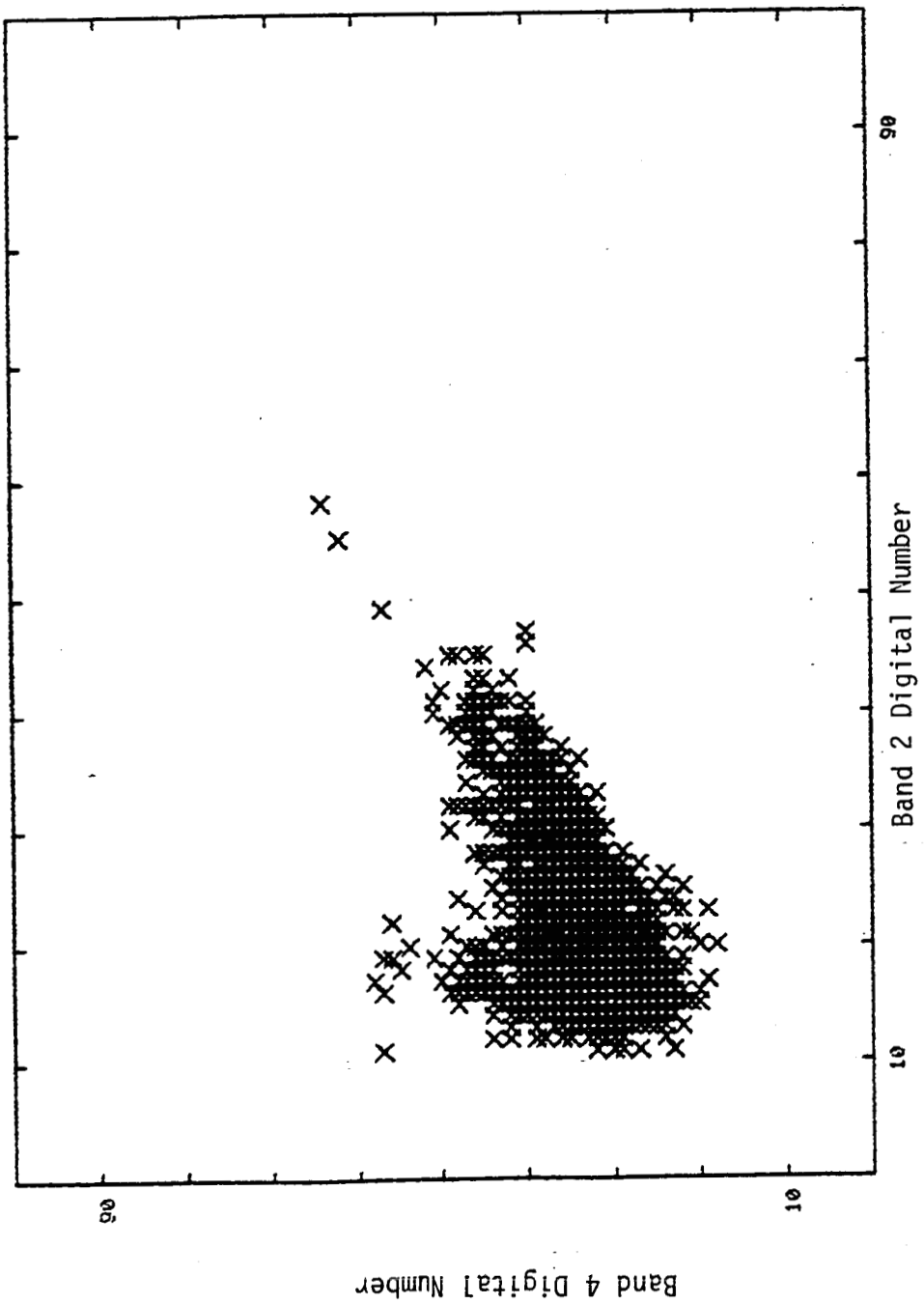

Data Plot of MSS Band 4 vs. Band 2
Segment of Foothills Region of Taos Study Area (2250 pixels)

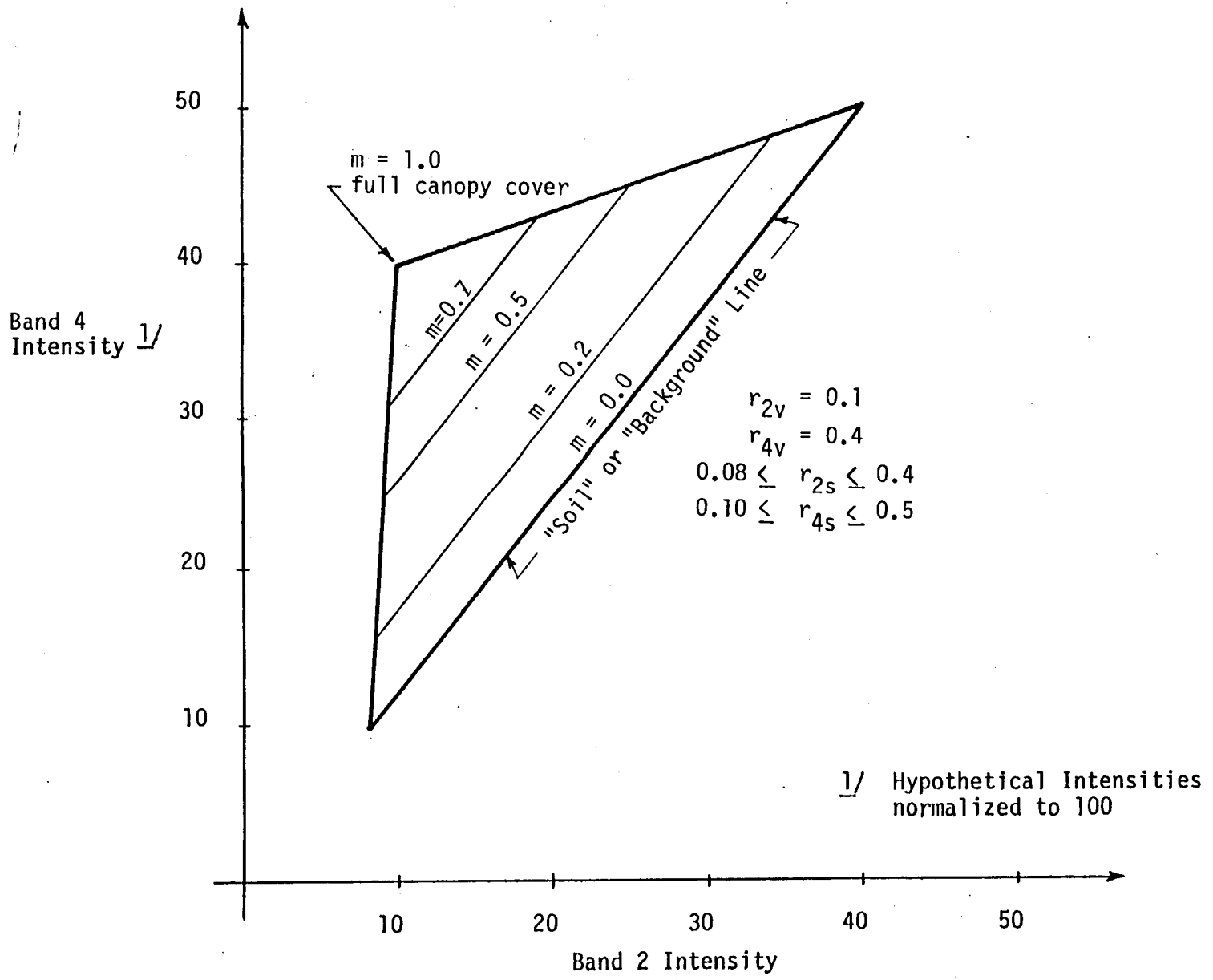

Hypothetical Data Space of Single Vegetation Species Landscape

Exhibit 5

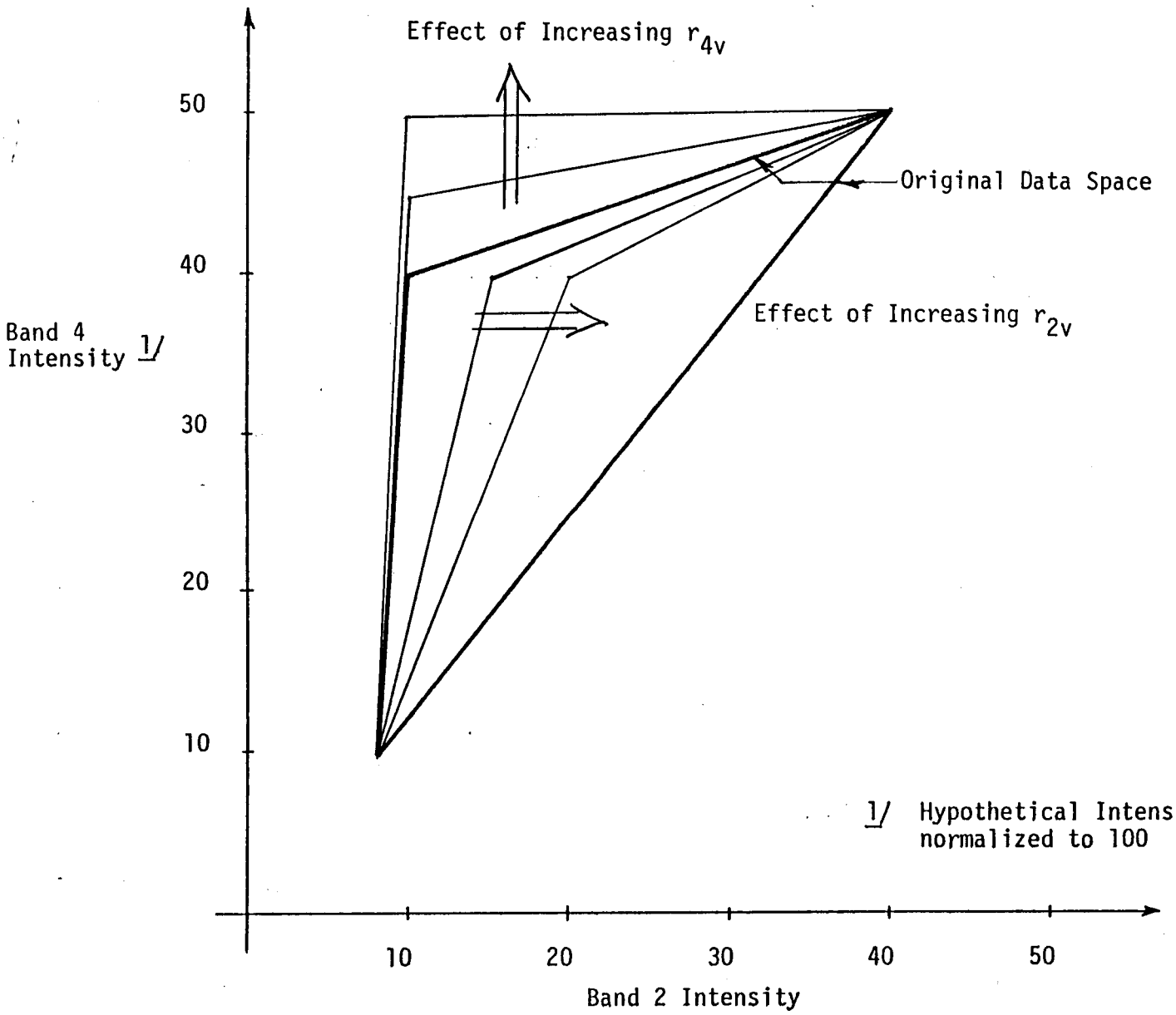

Effect of Increasing Vegetation Reflectivity on Hypothetical Data Space

Exhibit 6

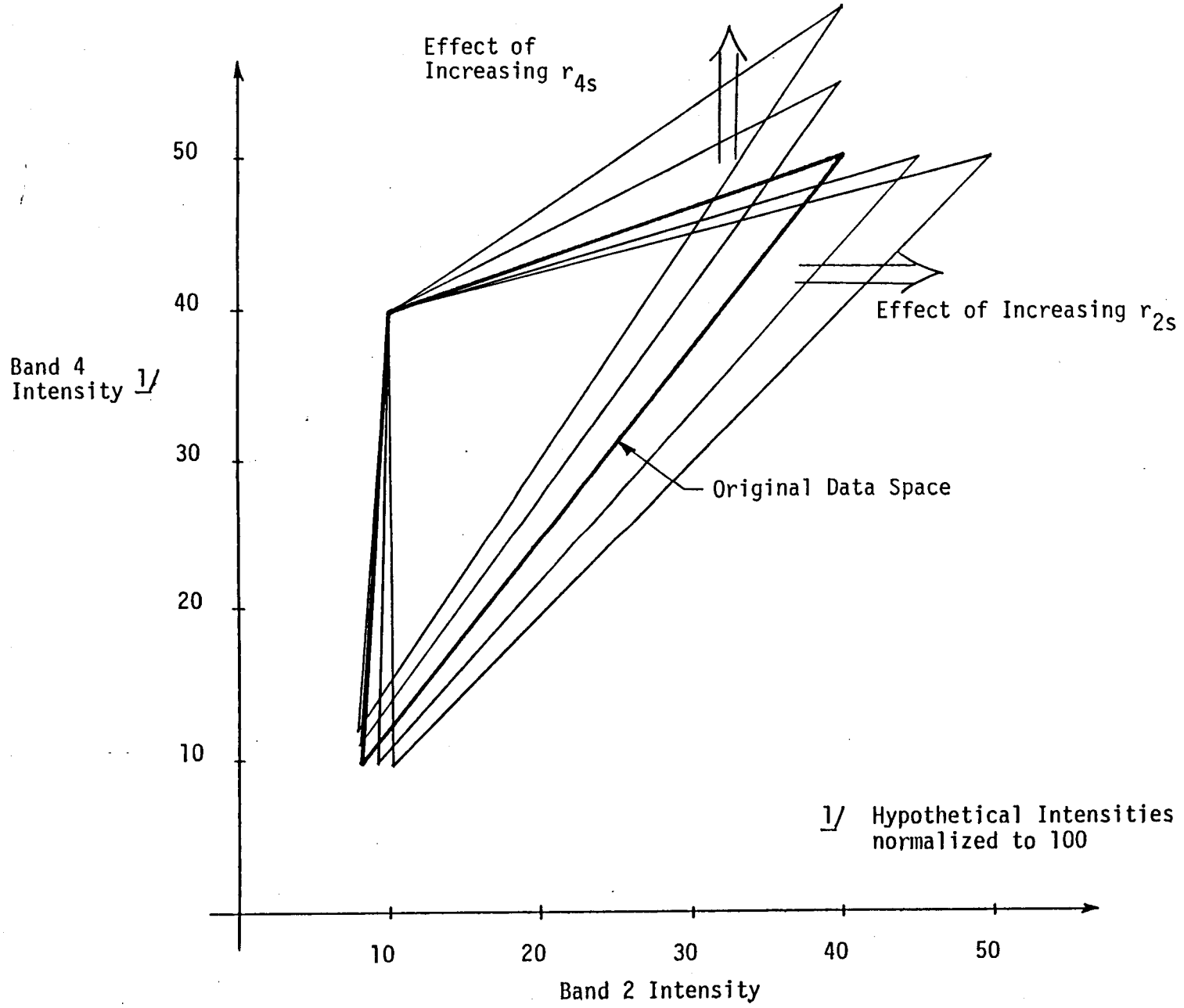

Effect of Increasing Soil Reflectivity on Hypothetical Data Space

Exhibit 7

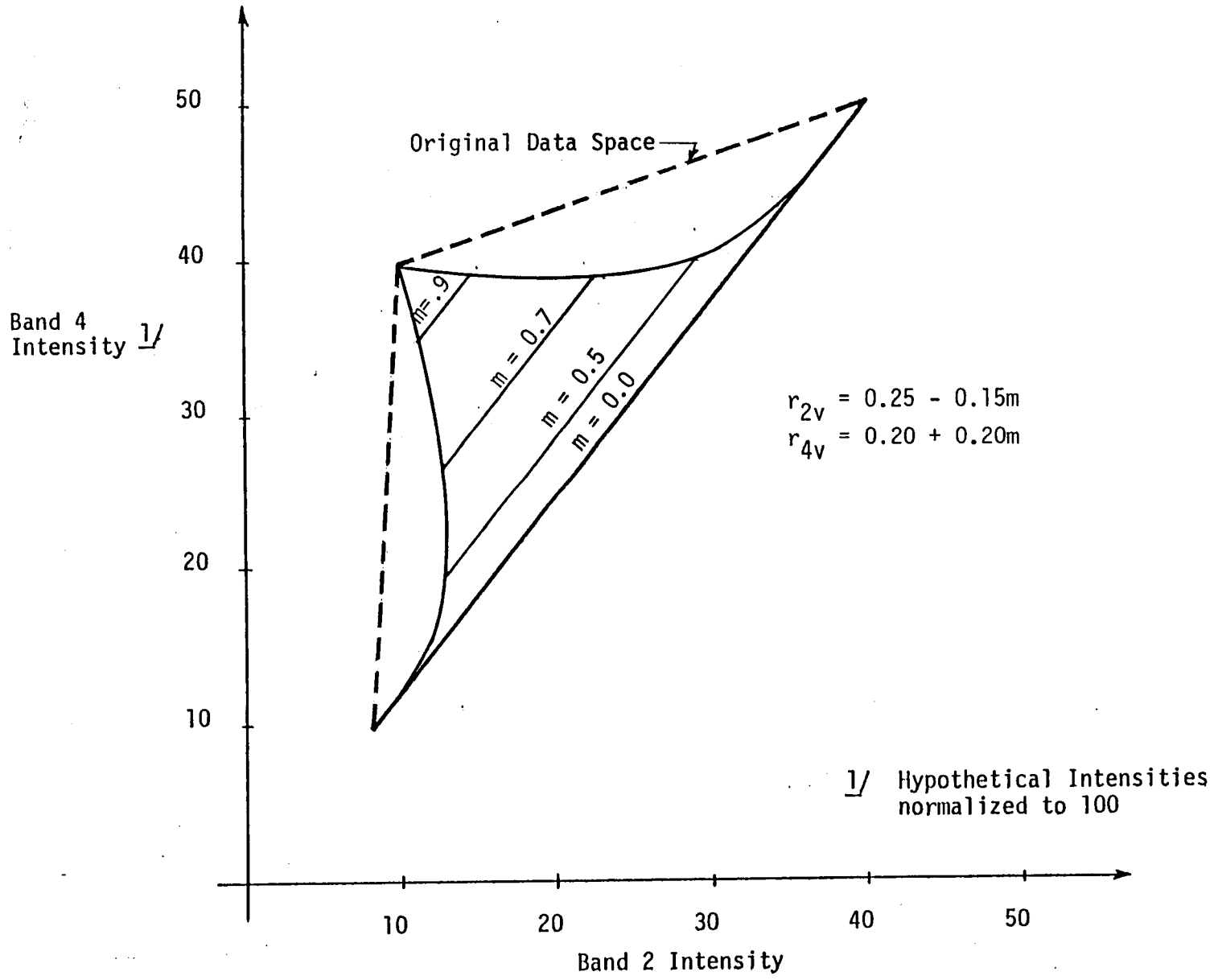

Effect of Variable Vegetation Reflectivity on Hypothetical Data Space

Exhibit 8

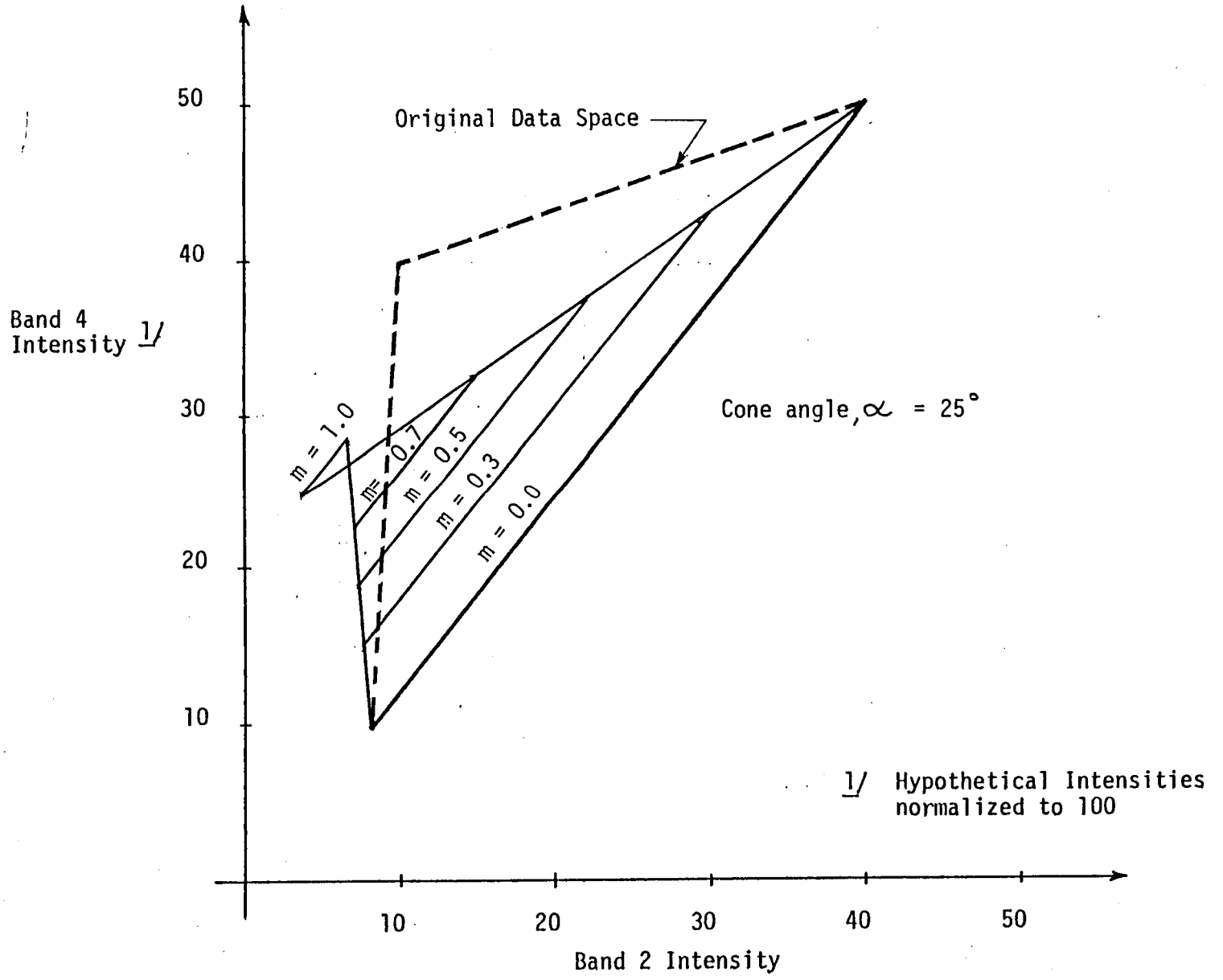

Effect of Shadows Cast by Cones on Hypothetical Data Space

Exhibit 9

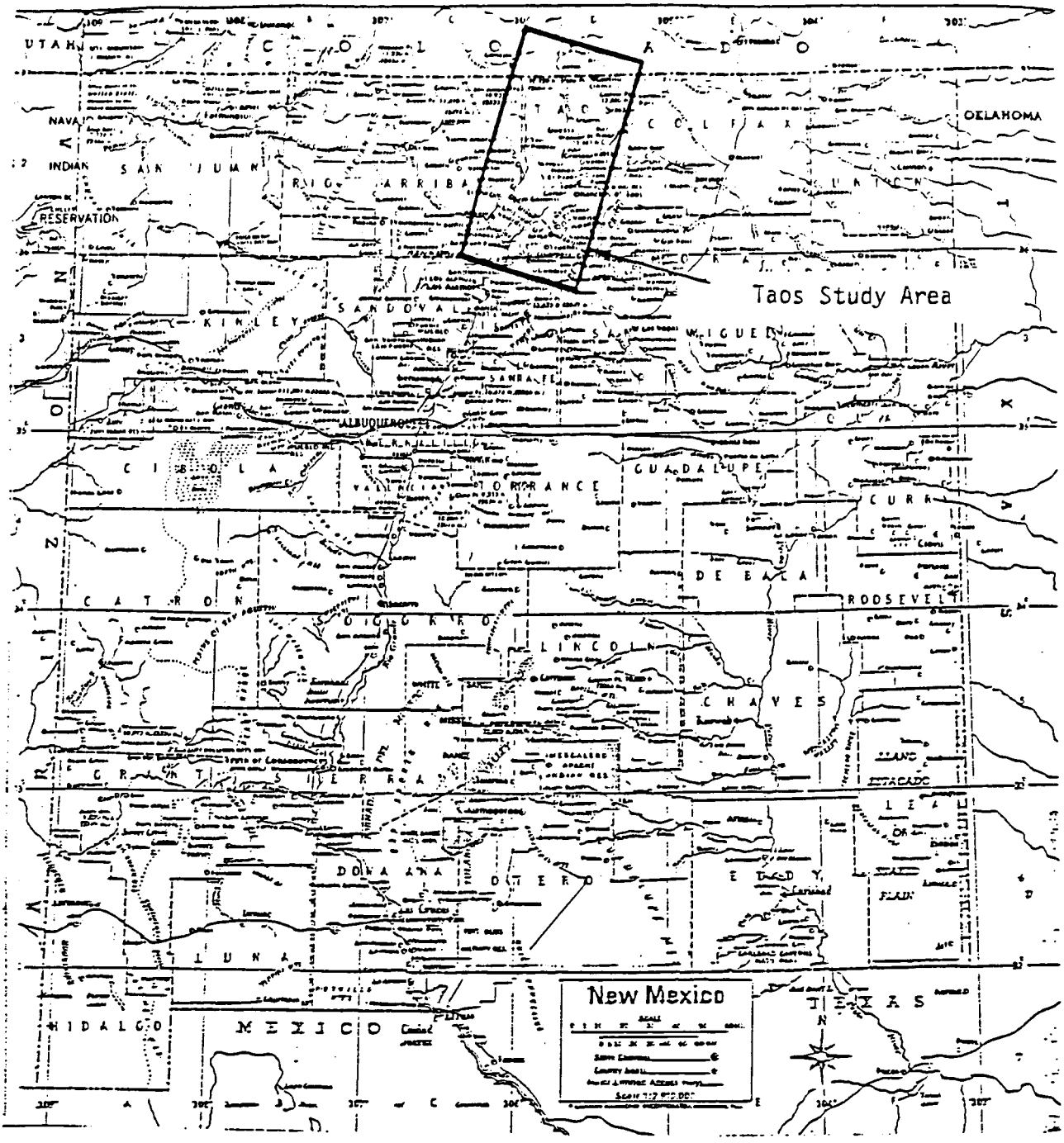

Location Map

Taos Study Area

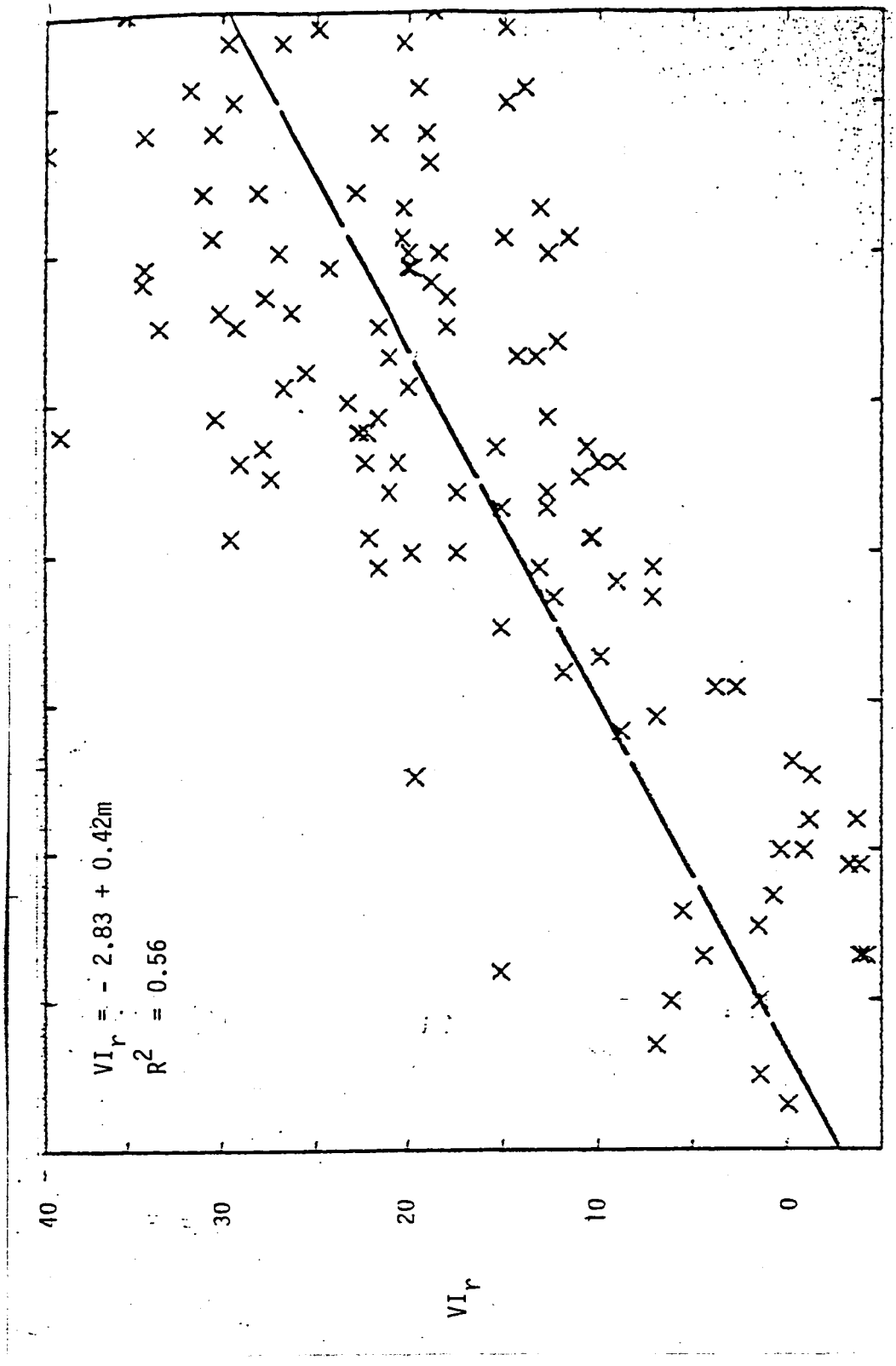

VI_r vs. Percent Green Canopy Cover

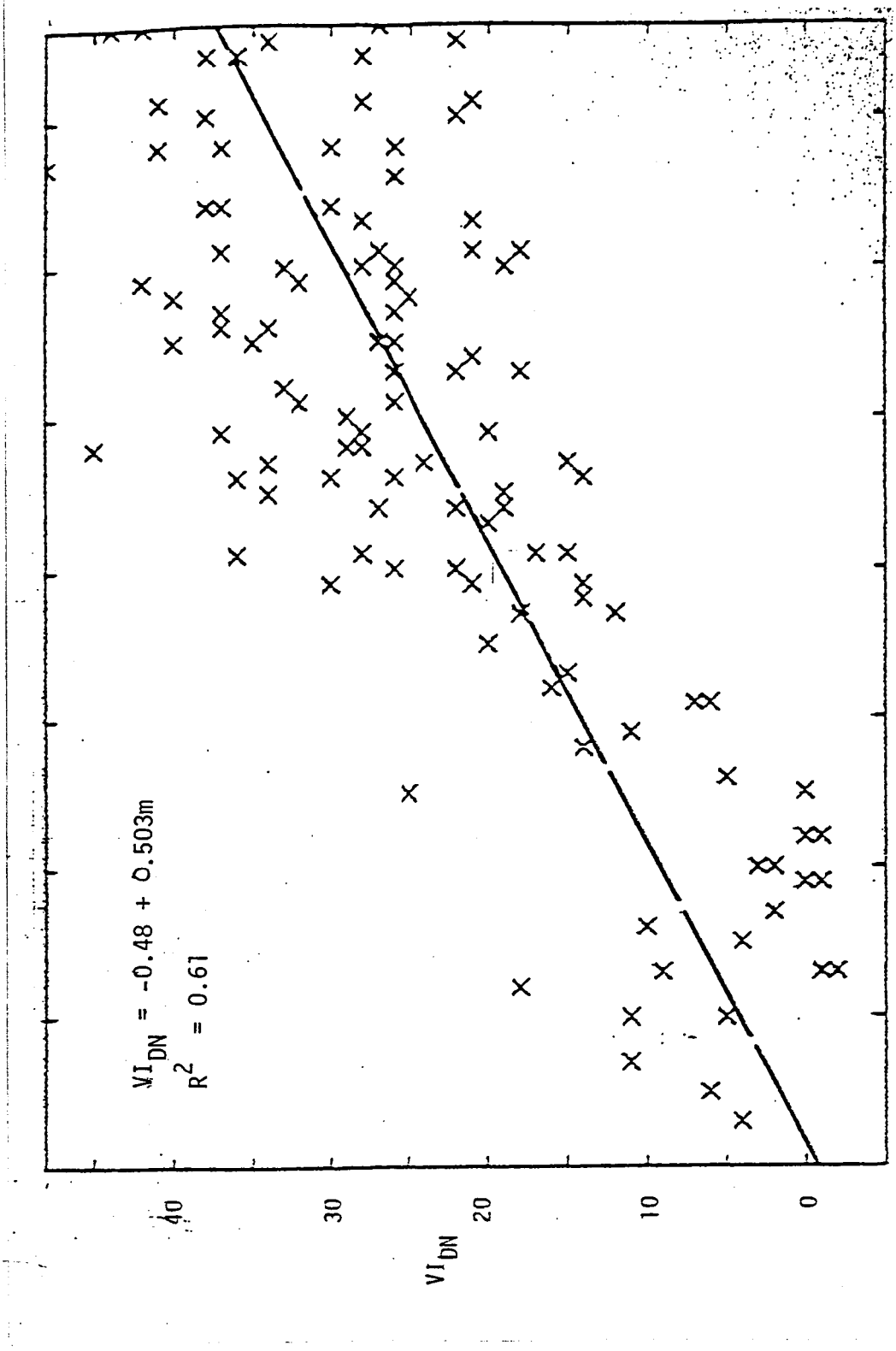

VI_{DN} vs. Percent Green Canopy Cover

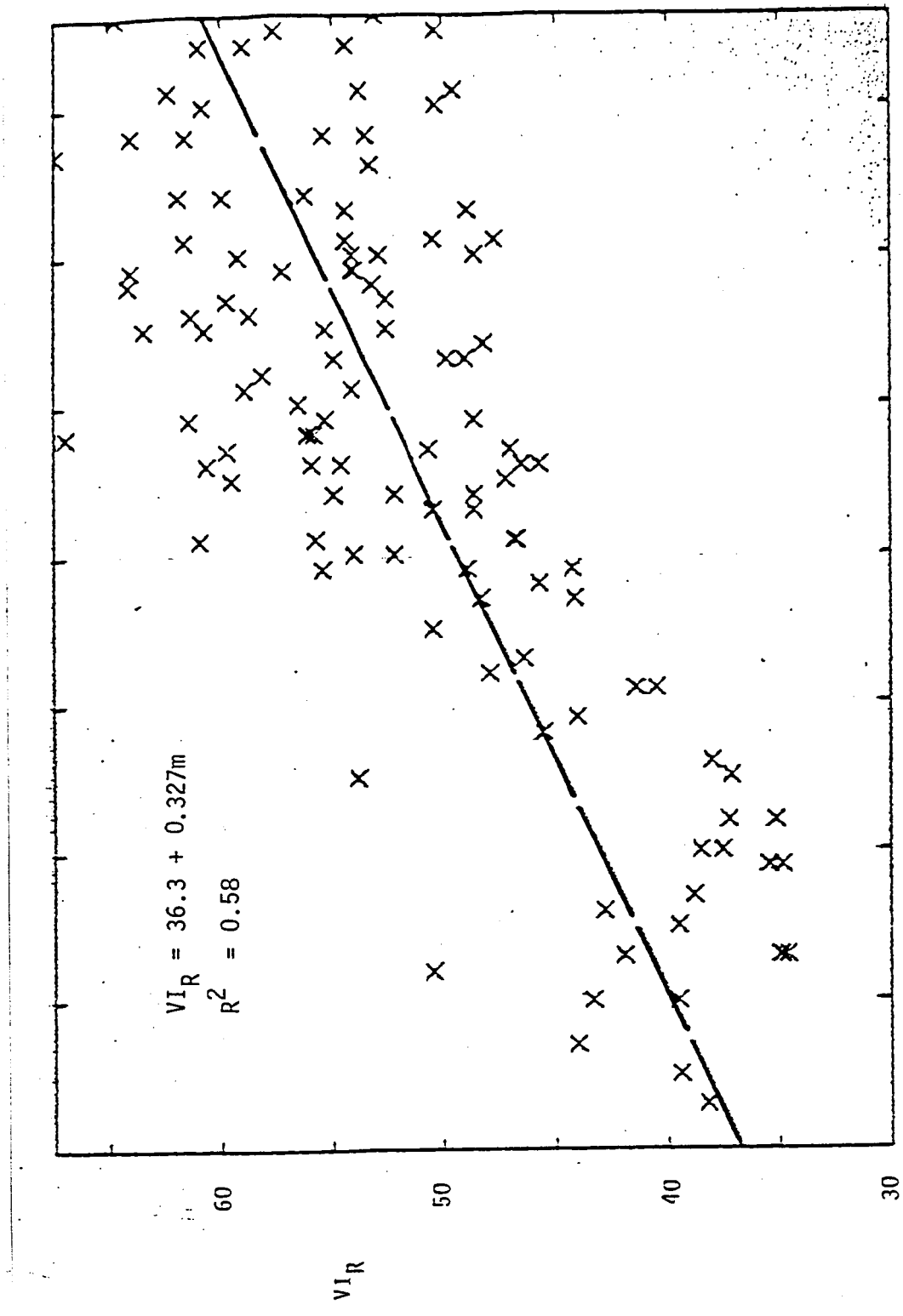

VI_R vs. Percent Green Canopy Cover

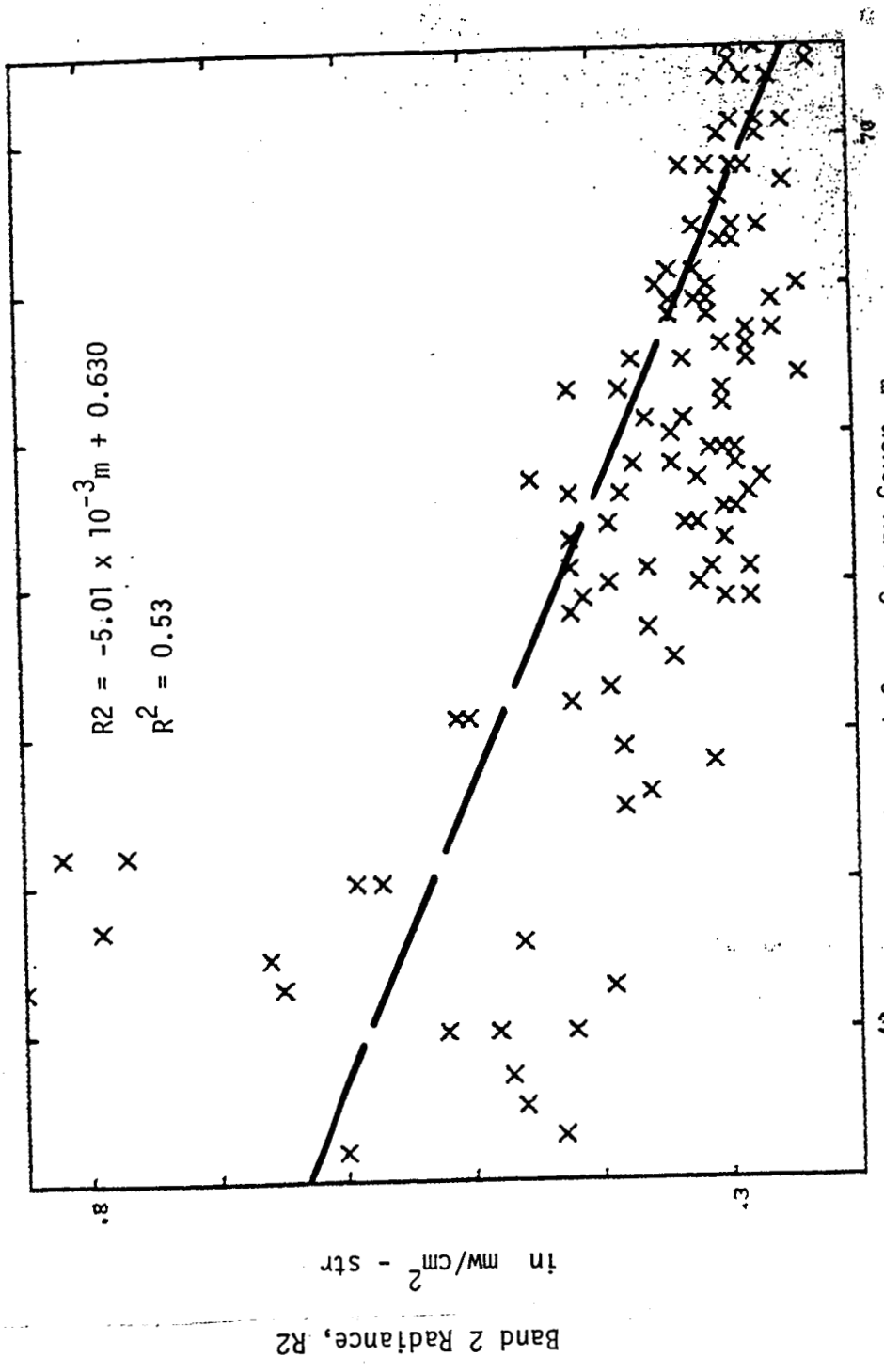

Band 2 Radiance vs. Percent Green Canopy Cover

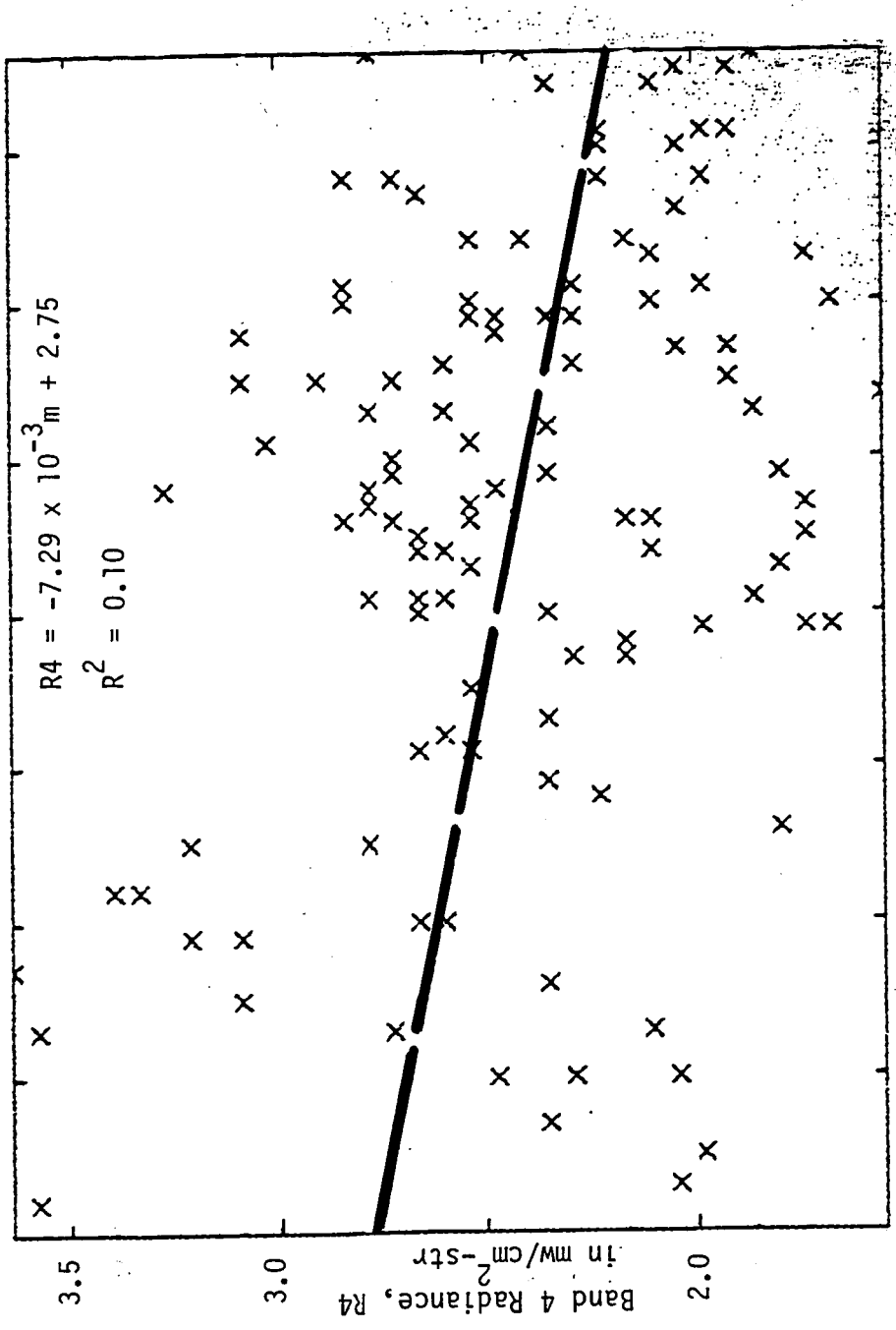

Band 4 Radiance vs. Percent Green Canopy Cover

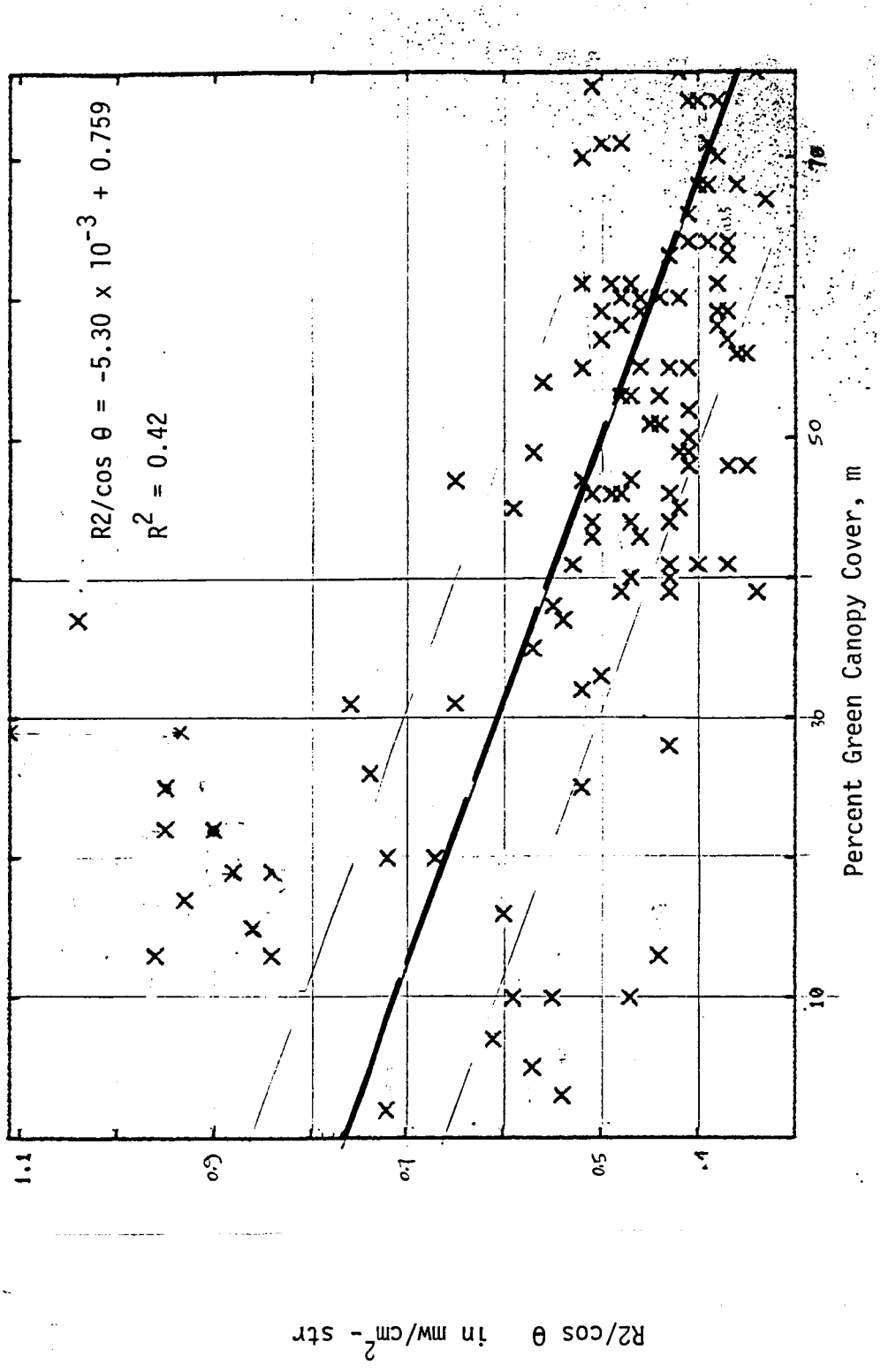

R2/cos θ vs Percent Green Canopy Cover

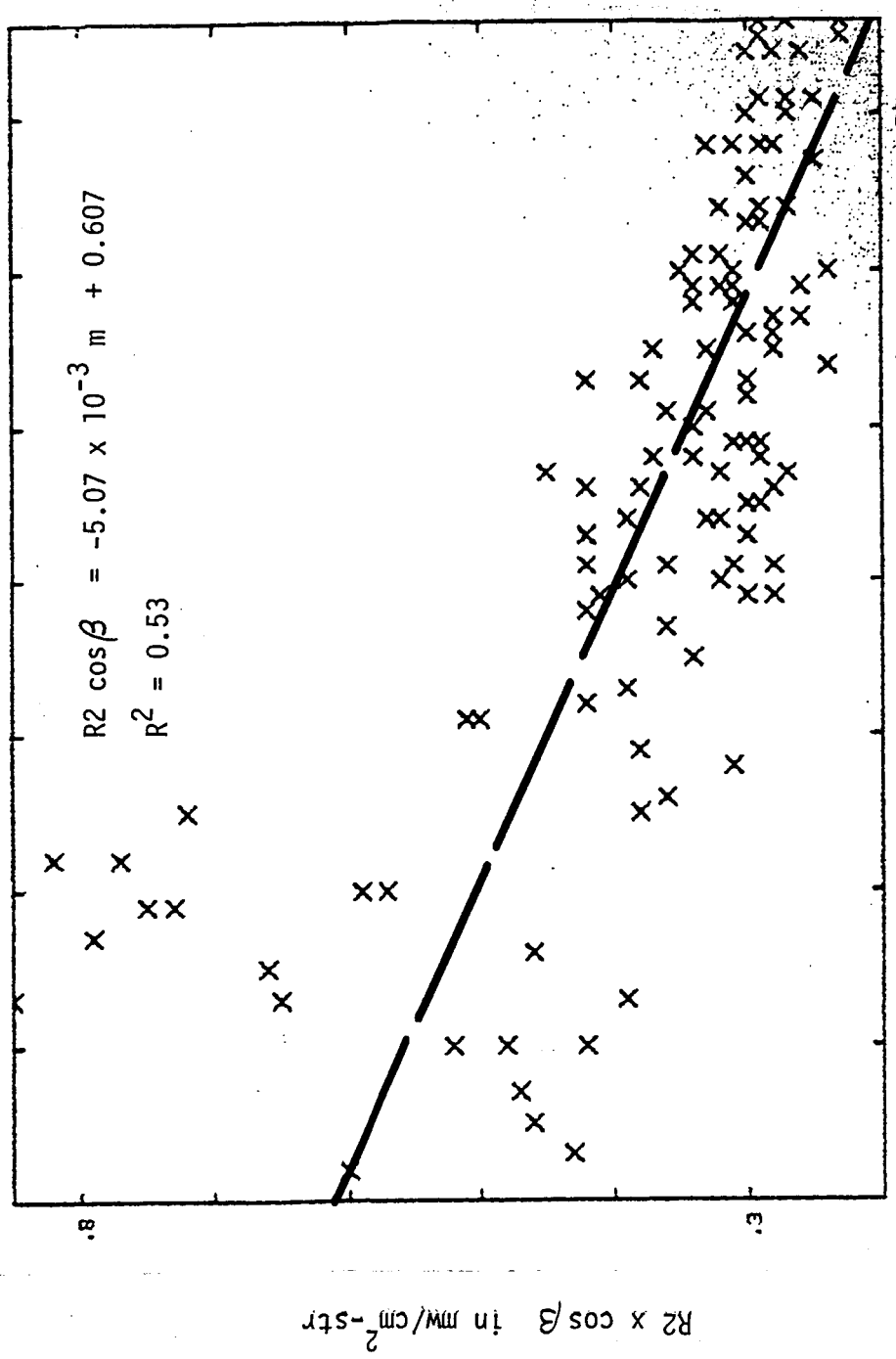

R2 cosβ vs. Percent Green Canopy Cover

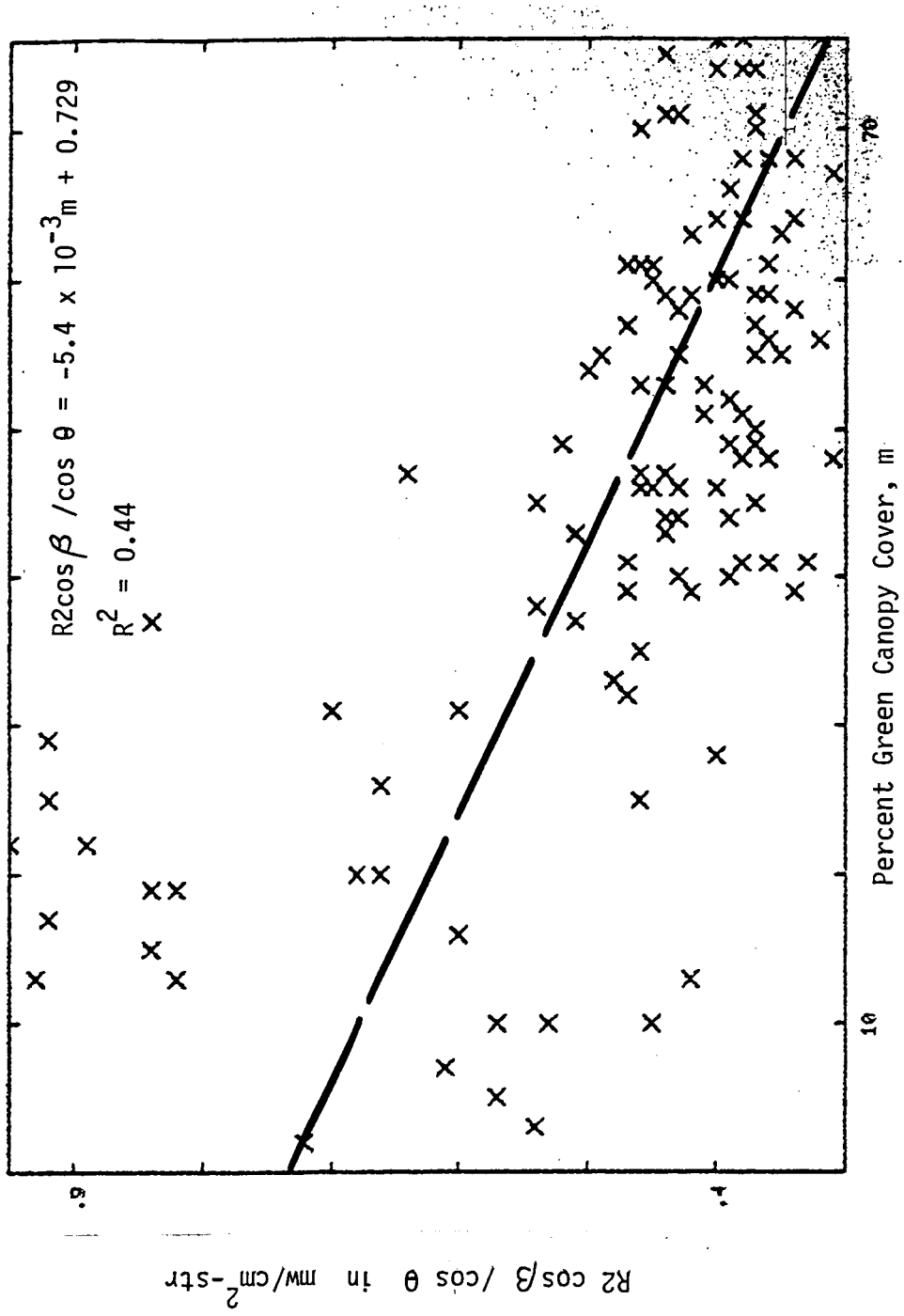

R2 cosβ /cos θ vs. Percent Green Canopy Cover

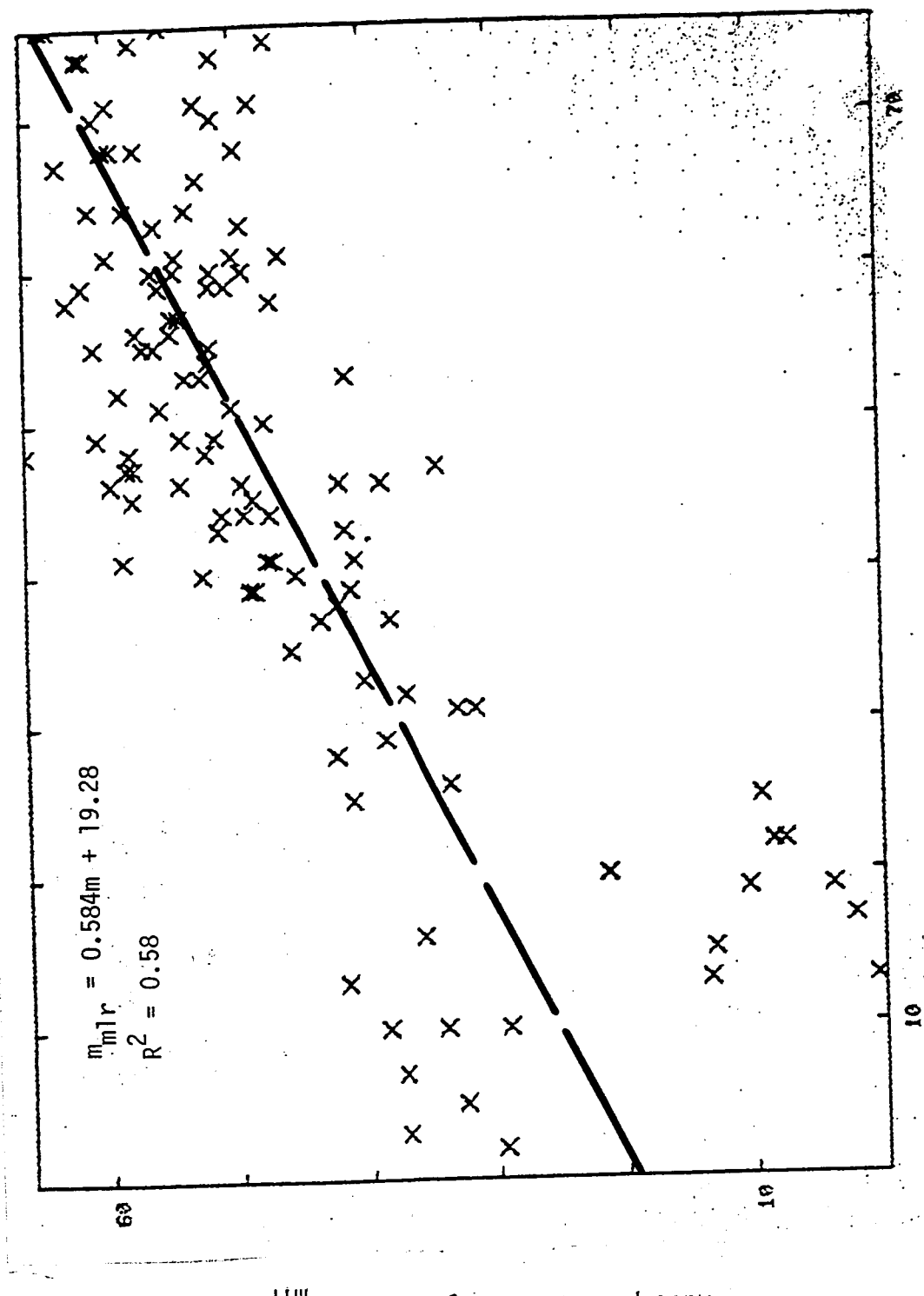

Percent Cover from Multiple Linear Regression vs. Actual Percent Cover

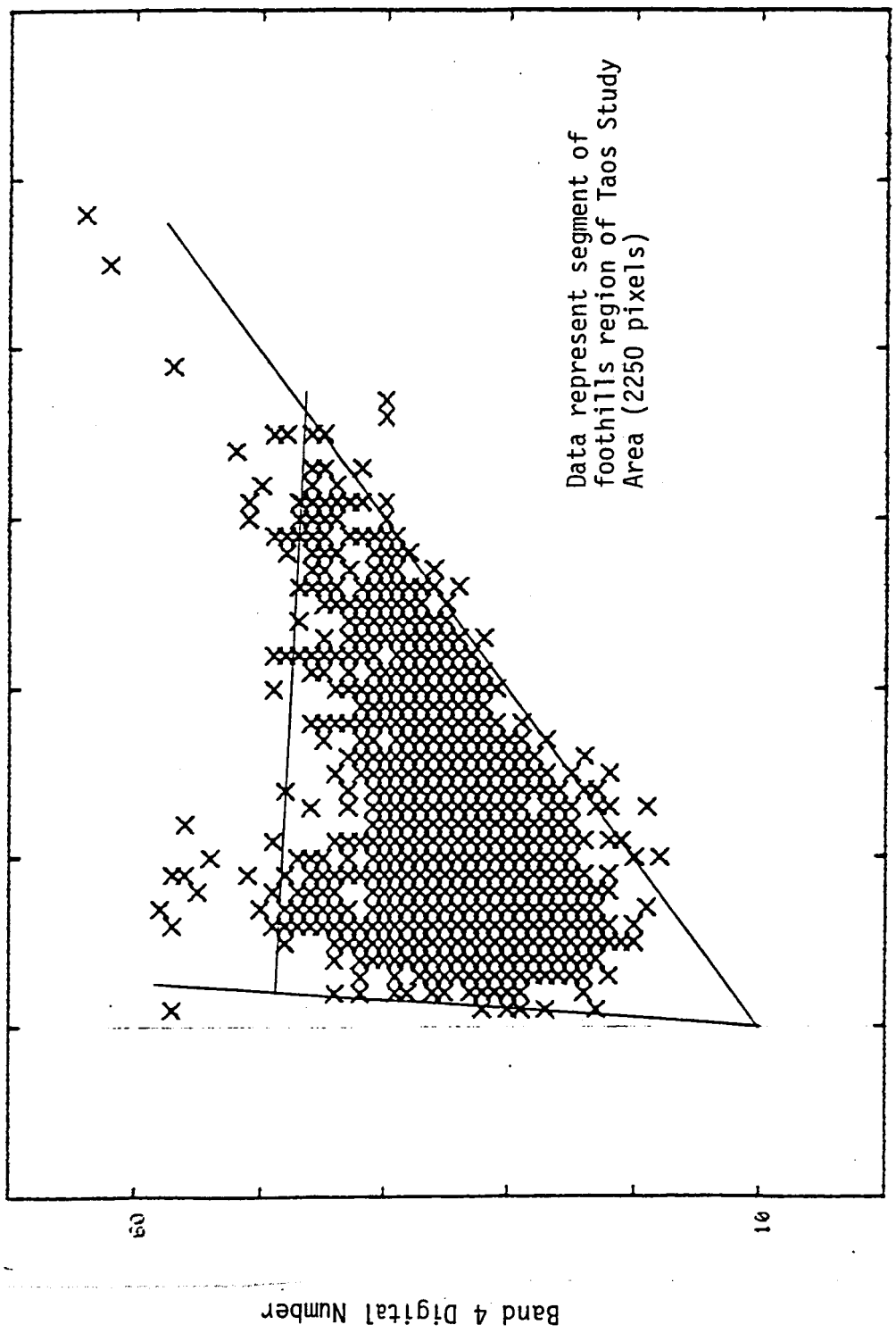

Data Plot of MSS Band 4 vs. Band 2
with Straight Envelope Lines

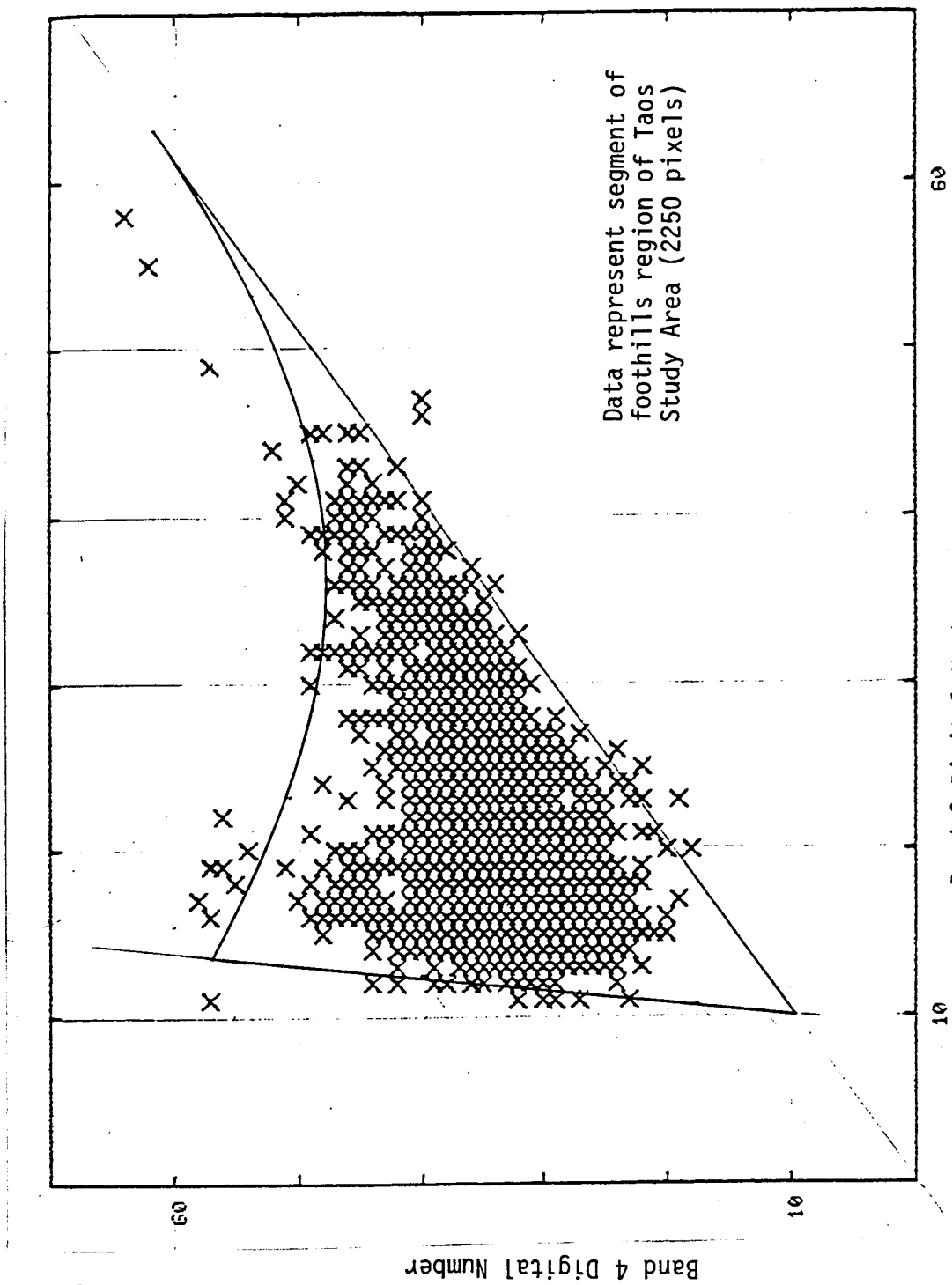

Data Plot of MSS Band 4 vs. Band 2
with Curved Envelope Lines

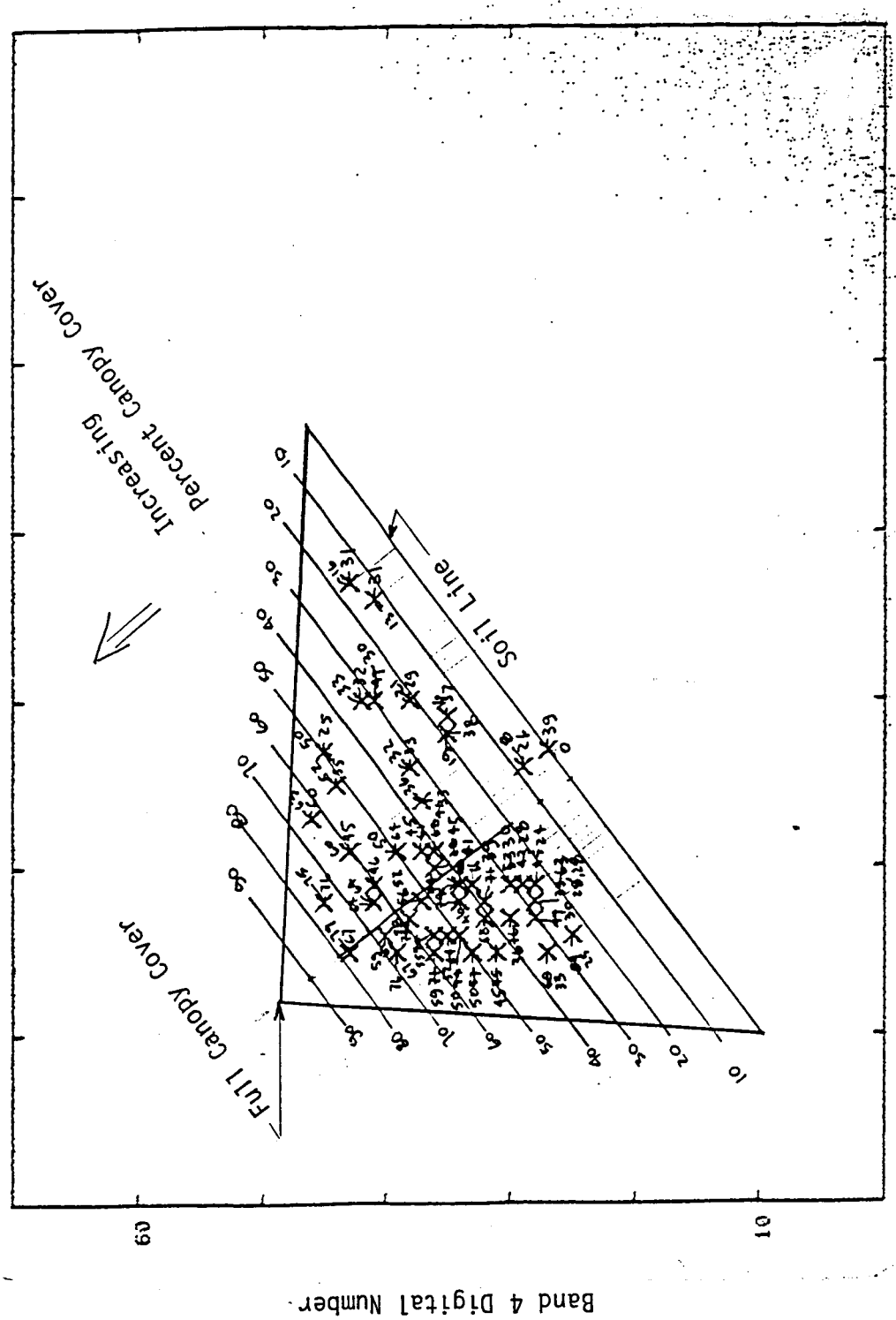

Data Plot of MSS Band 4 vs. Band 2 for Pixels with Ground Truth
Constant Vegetation Reflectivity Assumption

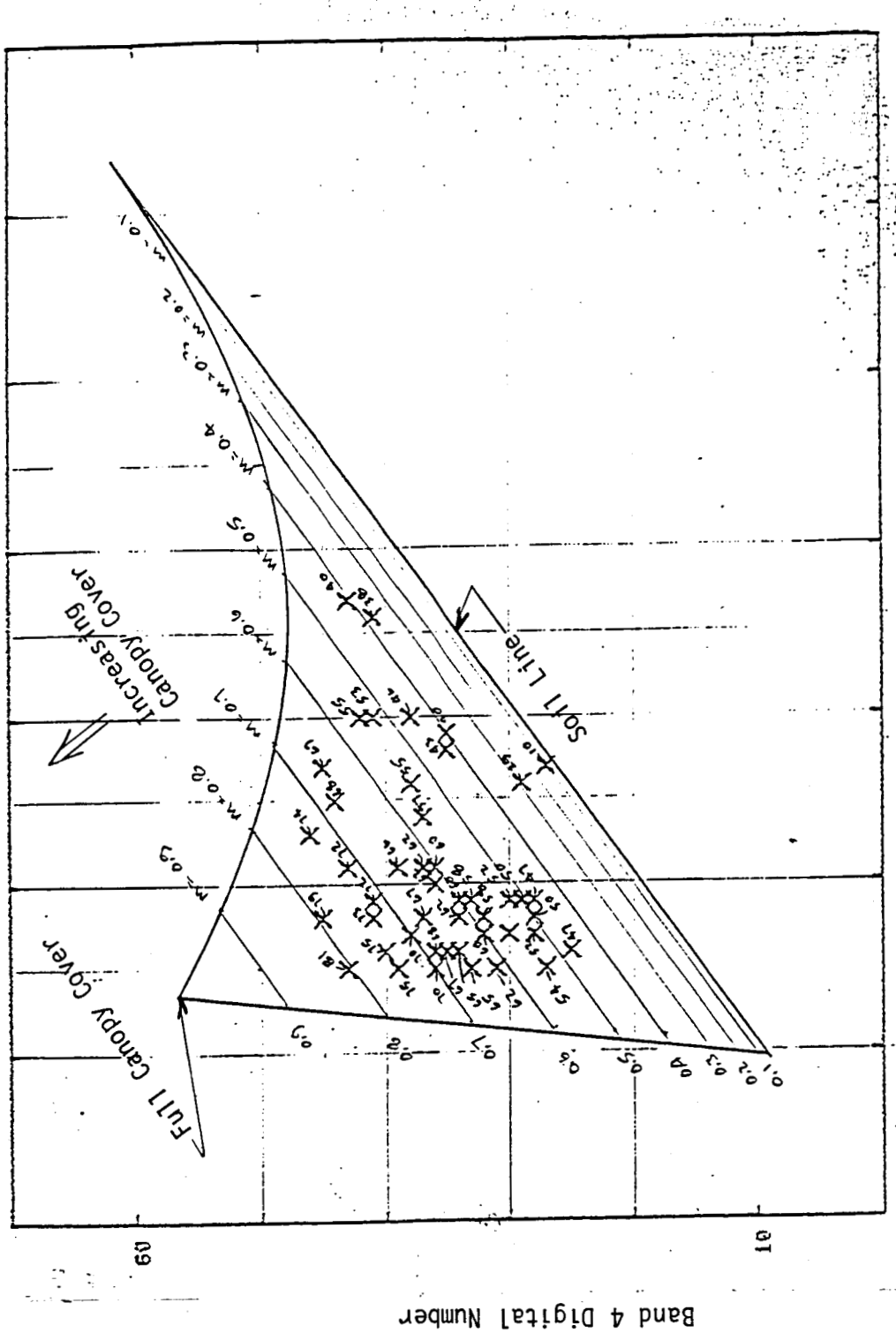

Data Plot of MSS Band 4 vs. Band 2 for Pixels with Ground Truth
Variable Vegetation Reflectivity Assumption

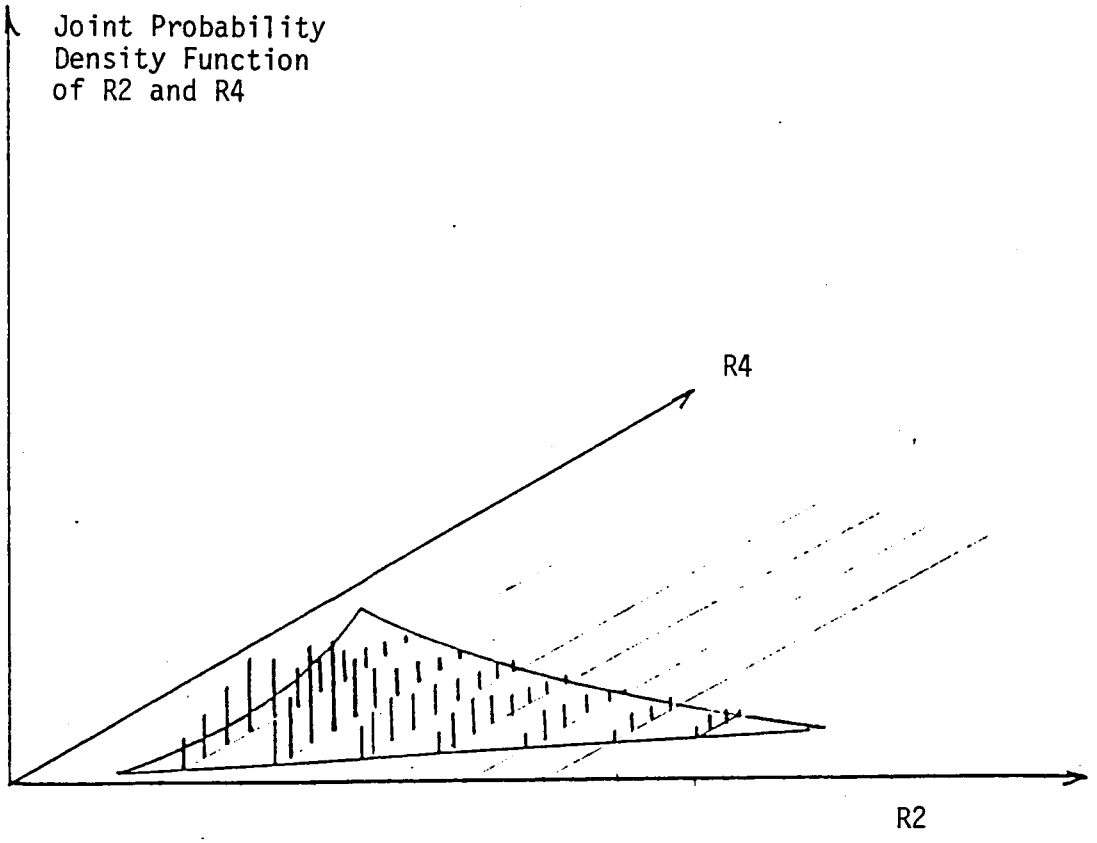

Hypothetical Joint Probability Density Function of R2 and R4